

Quantum Fisher information on two manifolds of two-mode Gaussian states

Paulina Marian^{1,2*} and Tudor A. Marian^{1†}

¹*Centre for Advanced Quantum Physics, Department of Physics,
University of Bucharest, R-077125 Bucharest-Măgurele, Romania and*

²*Department of Physical Chemistry, University of Bucharest,
Boulevard Regina Elisabeta 4-12, R-030018 Bucharest, Romania*

(Dated: August 30, 2018)

We investigate two special classes of two-mode Gaussian states of light that are important from both the experimental and theoretical points of view: the mode-mixed thermal states and the squeezed thermal ones. Aiming to a parallel study, we write the Uhlmann fidelity between pairs of states belonging to each class in terms of their defining parameters. The quantum Fisher information matrices on the corresponding four-dimensional manifolds are diagonal and allow insightful parameter estimation. The scalar curvatures of the Bures metric on both Riemannian manifolds of special two-mode Gaussian states are evaluated and discussed. They are functions of two variables, namely, the mean numbers of photons in the incident thermal modes. Our comparative analysis opens the door to further investigation of the interplay between geometry and statistics for Gaussian states produced in simple optical devices.

PACS numbers: 03.67.-a, 42.50.Dv, 02.40.Ky

I. INTRODUCTION

Answering the question "How close are two states of a quantum system?" is basic to the theory of quantum information processing. In principle, the similarity of states is decided via quantum-mechanical measurements whose outcomes are random, but have definite state-dependent probability distributions. There are several distance-type measures which are widely used to quantify the probabilistic distinguishability of two states [1, 2]. However, in this paper we focus on the most convenient of them, namely, the Bures distance that is defined in connection with quantum fidelity. Besides, the Bures metric for neighbouring states is proportional to the quantum Fisher information (QFI) metric known to be an essential ingredient in quantum metrology.

On the other hand, our paper deals with two-mode Gaussian states (GSs) of the quantum radiation field. There are two reasons for this choice. First, GSs are very useful tools in many quantum optics experiments. Some of them are interwoven with quantum information tasks. As an example, we mention that several quantum teleportation experiments were performed employing only GSs, starting with the first one carried out by Furusawa *et al.* [3]. On the theoretical side, the GSs of continuous-variable systems have been intensely investigated in the last three decades. Excellent recent reviews cover research on their role in quantum optics [4] and in quantum information as well [5, 6].

Second, exact explicit formulae have been found for the quantum fidelity of arbitrary one-mode [7] and two-mode GSs [8]. These available compact-form expressions are adequate for various calculations. In particular, they

allow one a straightforward derivation of the QFI metric for the one- and two-mode GSs. In what follows, we address this issue by exploiting the fidelity between two-mode GSs. More specifically, we make a parallel analysis for two classes of such states that are interesting in both experimental and theoretical research.

Below is presented the outline of the paper in some detail. In Sec. II, we start from the analogy between a classical probability distribution and that of the outcomes of a quantum-mechanical measurement. We recall the definition of the quantum fidelity between two states of a quantum system, its connection with their Bures distance, as well as the Uhlmann concise formula. Emphasis is laid on the proportionality of the infinitesimal Bures distance between neighbouring states to their QFI one. In Sec. III, we cast the expression of the fidelity between two arbitrary two-mode GSs [8] into an alternative form which seems to be more suitable for subsequent calculations. Section IV examines two important families of two-mode GSs, namely, the mode-mixed thermal states (MTSS) and the squeezed thermal states (STSS). We briefly review their optical generation, as well as their quantum-mechanical description. Despite some formal similarities in their natural parametrizations, their physical properties are quite different. However, this analysis has led us to term them special two-mode GSs and has suggested that a parallel investigation of their closeness features would be appropriate. By applying our alternative formula for the fidelity of two-mode GSs, we find in Sec. V the fidelity between MTSS and that between STSS, expressed in terms of their specific parameters. Section VI is devoted to the derivation of the QFI metric tensors on the four-dimensional Riemannian manifolds of the MTSS and STSS. Taking advantage that both natural parametrizations are orthogonal ones, we evaluate in Sec. VII the scalar curvature of the Bures metric on each Riemannian manifold of special two-mode GSs. The scalar

* paulina.marian@g.unibuc.ro

† tudor.marian@g.unibuc.ro

curvatures of all the MTSs and STSs depend only on their average numbers of photons in the incident thermal modes. We explain this specific property along with an alternative way of deriving both scalar curvatures. Their parallel presentation offers the possibility of some interesting comparisons. Section VIII summarizes the results and then gives a reliable statistical interpretation of the Riemannian scalar curvature based on the Bures metric. Three appendices detail two basic inequalities involving fidelity in the particular case of GSs. Appendix A deals with the inequality between the fidelity and the overlap of two n -mode GSs. In Appendix B, the property of fidelity of being less than one or at most equal to one is checked for thermal states (TSs). Explicit use of this conclusion is made in Appendix C in order to verify the same inequality for two-mode MTSs and STSs.

II. QUANTUM FIDELITY

To start on, let $P := \{p_b\}$, ($b = 1, \dots, N$), denote a probability distribution assigned to the sample space of an experiment with N outcomes. We consider two arbitrary probability distributions, $P' := \{p'_b\}$ and $P'' := \{p''_b\}$, ascribed to the given sample space. Their classical fidelity is the square of the scalar product of two unit vectors in \mathbb{R}^N with the components $\{\sqrt{p'_b}\}$ and $\{\sqrt{p''_b}\}$:

$$\mathcal{F}_{cl}(P', P'') := \left(\sum_{b=1}^N \sqrt{p'_b p''_b} \right)^2. \quad (2.1)$$

These vectors define two points on a hyperoctant of the unit sphere S^{N-1} embedded in the Euclidean space \mathbb{R}^N . Their angle at the center of the sphere [9, 10] is called the Bhattacharyya-Wootters statistical distance [11]:

$$D_{BW}(P', P'') := \arccos \left(\sqrt{\mathcal{F}_{cl}(P', P'')} \right). \quad (2.2)$$

The square root of the classical fidelity is referred to as affinity of the probability distributions [12]. Note that the Hellinger distance between the points P' and P'' [12],

$$D_H(P', P'') := \left[\sum_{b=1}^N \left(\sqrt{p'_b} - \sqrt{p''_b} \right)^2 \right]^{\frac{1}{2}}, \quad (2.3)$$

coincides with their chordal distance and is in turn determined by the classical fidelity (2.1):

$$D_H(P', P'') = \left[2 - 2\sqrt{\mathcal{F}_{cl}(P', P'')} \right]^{\frac{1}{2}}. \quad (2.4)$$

In order to estimate the closeness of two arbitrary states, $\hat{\rho}'$ and $\hat{\rho}''$, of a given quantum system, Bures introduced a distance between them [13] which is similar to the classical Hellinger distance (2.4):

$$D_B(\hat{\rho}', \hat{\rho}'') := \left[2 - 2\sqrt{\mathcal{F}(\hat{\rho}', \hat{\rho}'')} \right]^{\frac{1}{2}}. \quad (2.5)$$

Let \mathcal{H} denote the Hilbert space associated to the quantum system. The quantity $\mathcal{F}(\hat{\rho}', \hat{\rho}'')$ occurring in Eq. (2.5) is defined as the maximal transition probability between any pair of purifications of the states $\hat{\rho}'$ and $\hat{\rho}''$. However, it is sufficient to restrict our choice of purifications to pairs of state vectors, $|\Psi'\rangle$ and $|\Psi''\rangle$, both belonging to the tensor product space $\mathcal{H} \otimes \mathcal{H}$:

$$\mathcal{F}(\hat{\rho}', \hat{\rho}'') := \max_{\{|\Psi'\rangle, |\Psi''\rangle\}} |\langle \Psi' | \Psi'' \rangle|^2. \quad (2.6)$$

Subsequently [14], Uhlmann succeeded in deriving the compact expression

$$\mathcal{F}(\hat{\rho}', \hat{\rho}'') = \left[\text{Tr} \left(\sqrt{\sqrt{\hat{\rho}''} \hat{\rho}' \sqrt{\hat{\rho}''}} \right) \right]^2 \quad (2.7)$$

and interpreted it as a *generalization* of the quantum-mechanical transition probability between the above states. In a later paper [15], Jozsa coined the name *fidelity* for the non-negative quantity (2.7) and gave elementary proofs of its main properties. Note that, when at least one of the quantum states is pure, the fidelity (2.7) reduces to the Hilbert-Schmidt scalar product of the states: $\mathcal{F}(\hat{\rho}', \hat{\rho}'') = \text{Tr}(\hat{\rho}' \hat{\rho}'')$. Let us assume, for instance, that $\hat{\rho}''$ is a pure state, i. e., $\hat{\rho}'' = |\psi''\rangle\langle\psi''|$, while the state $\hat{\rho}'$ is either pure or mixed. Then their fidelity,

$$\mathcal{F}(\hat{\rho}', |\psi''\rangle\langle\psi''|) = \langle \psi'' | \hat{\rho}' | \psi'' \rangle, \quad (2.8)$$

is the probability of transforming the state $\hat{\rho}'$ into the state $\hat{\rho}'' = |\psi''\rangle\langle\psi''|$ via a selective measurement. By contrast, the fidelity (2.7) has no such operational meaning when both states are mixed ones. In this general case, its probabilistic significance relies merely on the Bures-Uhlmann definition (2.6).

We mention three properties of the fidelity that are displayed by Eq. (2.6).

1) Fidelity is less than one or at most equal to one. This inequality saturates if and only if the states coincide:

$$\mathcal{F}(\hat{\rho}', \hat{\rho}'') \leq 1: \quad \mathcal{F}(\hat{\rho}', \hat{\rho}'') = 1 \iff \hat{\rho}'' = \hat{\rho}'. \quad (2.9)$$

2) Symmetry:

$$\mathcal{F}(\hat{\rho}'', \hat{\rho}') = \mathcal{F}(\hat{\rho}', \hat{\rho}''). \quad (2.10)$$

3) Monotonicity. Fidelity doesn't decrease under any trace-preserving quantum operation \mathcal{E} performed on both states [1]:

$$\mathcal{F}(\mathcal{E}(\hat{\rho}'), \mathcal{E}(\hat{\rho}'')) \geq \mathcal{F}(\hat{\rho}', \hat{\rho}''). \quad (2.11)$$

Besides, fidelity proved to be an appropriate indicator of the closeness of two quantum states via measurements. Recall that for any general measurement there is a Positive Operator-Valued Measure (POVM) [1], i. e., a set of positive operators $\{\hat{E}_b\}$ on the Hilbert space \mathcal{H} , which provides a resolution of the identity: $\sum_b \hat{E}_b = \hat{I}$. The

subscript b indexes the possible outcomes of the measurement whose probabilities in the quantum states $\hat{\rho}'$ and $\hat{\rho}''$ are, respectively, $p_{\hat{\rho}'}(b) = \text{Tr}(\hat{\rho}' \hat{E}_b)$ and $p_{\hat{\rho}''}(b) = \text{Tr}(\hat{\rho}'' \hat{E}_b)$. One can extend the formula (2.1) to define the classical fidelity of these probability distributions in a given quantum measurement:

$$\mathcal{F}_{cl}(p_{\hat{\rho}'}, p_{\hat{\rho}''}; \{\hat{E}_b\}) := \left[\sum_b \sqrt{p_{\hat{\rho}'}(b) p_{\hat{\rho}''}(b)} \right]^2. \quad (2.12)$$

In Refs. [11, 16, 17] it was proven an important theorem stating that the quantum fidelity is the minimal classical one (2.12) over the collection of all POVMs:

$$\mathcal{F}(\hat{\rho}', \hat{\rho}'') = \min_{\{\hat{E}_b\}} \left[\mathcal{F}_{cl}(p_{\hat{\rho}'}, p_{\hat{\rho}''}; \{\hat{E}_b\}) \right]. \quad (2.13)$$

When the states $\hat{\rho}'$ and $\hat{\rho}''$ commute, then and only then their fidelity (2.7) is equal to the square of their quantum affinity [18]:

$$[\hat{\rho}', \hat{\rho}''] = \hat{0} \iff \mathcal{F}(\hat{\rho}', \hat{\rho}'') = \left[\text{Tr} \left(\sqrt{\hat{\rho}'} \sqrt{\hat{\rho}''} \right) \right]^2. \quad (2.14)$$

The spectral resolutions of the commuting density operators $\hat{\rho}'$ and $\hat{\rho}''$ are written in terms of the same complete set of orthogonal projections, albeit with specific spectra: $\{\lambda'_n\}$ and $\{\lambda''_n\}$, respectively. Therefore, Eq. (2.14) takes the form (2.12):

$$[\hat{\rho}', \hat{\rho}''] = \hat{0} \iff \mathcal{F}(\hat{\rho}', \hat{\rho}'') = \left(\sum_n \sqrt{\lambda'_n \lambda''_n} \right)^2. \quad (2.15)$$

Accordingly, in the properly termed *classical* situation of commuting states, the minimum (2.13) is reached for a clearly specified projective measurement.

We emphasize that, in the spirit of the correspondence principle, it is possible to *guess* the positive operator $\hat{\mathcal{B}} := \sqrt{\hat{\rho}''} \hat{\rho}' \sqrt{\hat{\rho}''}$ [8] occurring in the Uhlmann formula (2.7). Indeed, the above structure of $\hat{\mathcal{B}}$ is the simplest one which leads to the classical limit (2.15).

Another fidelity-based distance is the Bures angle [1],

$$D_A(\hat{\rho}', \hat{\rho}'') := \arccos \left(\sqrt{\mathcal{F}(\hat{\rho}', \hat{\rho}'')} \right). \quad (2.16)$$

On account of Eqs. (2.9) and (2.10), both the Bures distance and the Bures angle are genuine metrics since they fulfill in addition the triangle inequality, as shown in Refs. [13, 19] and, respectively, [1]. Moreover, by virtue of the monotonicity property (2.11) of the fidelity, they are contractive distances (monotone metrics).

Recall that the natural distance between two pure states, $|\psi'\rangle\langle\psi'|$ and $|\psi''\rangle\langle\psi''|$, on the manifold of the projective Hilbert space is the Fubini-Study metric [2]:

$$D_{\text{FS}}(|\psi'\rangle\langle\psi'|, |\psi''\rangle\langle\psi''|) := \arccos(|\langle\psi'|\psi''\rangle|). \quad (2.17)$$

The Bures angle (2.16) is just the generalization of the Fubini-Study metric to the case of mixed states.

We further concentrate on the squared Bures distance between two neighbouring quantum states denoted $\hat{\rho}$ and $\hat{\rho} + d\hat{\rho}$:

$$(ds_B)^2 := [D_B(\hat{\rho}, \hat{\rho} + d\hat{\rho})]^2. \quad (2.18)$$

The above squared infinitesimal line element is built with the Bures metric tensor on a certain differentiable manifold of quantum states. An important result of Uhlmann's school obtained long ago [20] is that the Bures metric (2.18) is Riemannian.

In a seminal paper [21], Braunstein and Caves employ the theory of parameter estimation to find the optimal quantum measurement that resolves two neighbouring mixed states. Thus they generalize the Wootters statistical distance between pure states [10]. These authors succeeded in deriving the QFI metric $(ds_F)^2$ as a reliable measure of statistical distinguishability between neighbouring quantum states. Furthermore, a comparison of the QFI metric with Hübner's general expression of the infinitesimal Bures metric [20] allowed them to establish the basic proportionality formula

$$(ds_B)^2 = \frac{1}{4} (ds_F)^2. \quad (2.19)$$

A pertinent analysis of the infinitesimal metric on any finite-dimensional state space is carried out in Ref. [22] and then carefully reviewed in Ref. [23]. It reveals a couple of distinctive features of the Bures metric (2.18). Specifically, this is the minimal one among the monotone, Riemannian, and Fisher-adjusted metrics. In addition, it is the only metric from the above class whose extension to pure states yields precisely the Fubini-Study metric.

III. UHLMANN FIDELITY BETWEEN TWO-MODE GAUSSIAN STATES

In order to tackle the two-mode GSs, we arrange the canonical quadrature operators of the modes in a row vector:

$$(\hat{u})^T := (\hat{q}_1, \hat{p}_1, \hat{q}_2, \hat{p}_2). \quad (3.1)$$

Their eigenvalues are the components of an arbitrary dimensionless vector $u \in \mathbb{R}^4$:

$$u^T := (q_1, p_1, q_2, p_2). \quad (3.2)$$

Recall that any GS $\hat{\rho}$ is defined by its characteristic function (CF) $\chi(u)$. In turn, this is fully determined by the first- and second-order moments of the quadrature operators (3.1) in the given state $\hat{\rho}$. As a matter of fact, the CF $\chi(u)$ is an exponential whose argument is a specific quadratic function of the current vector u , Eq. (3.2):

$$\chi(u) = \exp \left[-\frac{1}{2} (Ju)^T \mathcal{V} (Ju) + iv^T (Ju) \right]. \quad (3.3)$$

In Eq. (3.3), the components of the vector $v \in \mathbb{R}^4$ are the expectation values of the quadrature operators (3.1) in the chosen GS $\hat{\rho}$: $v := \langle \hat{u} \rangle_{\hat{\rho}}$. The second-order moments of the deviations from the means of the canonical quadrature operators are collected as entries of the real and symmetric 4×4 covariance matrix (CM) \mathcal{V} of the GS $\hat{\rho}$. In the sequel, we find it often useful to write the CM partitioned into the following 2×2 submatrices:

$$\mathcal{V} = \begin{pmatrix} \mathcal{V}_1 & \mathcal{C} \\ \mathcal{C}^T & \mathcal{V}_2 \end{pmatrix}. \quad (3.4)$$

The submatrices \mathcal{V}_j , ($j = 1, 2$), are the CMs of the single-mode reduced GSs, while \mathcal{C} displays the cross-correlations between the modes. Further, J denotes the standard 4×4 matrix of the symplectic form on \mathbb{R}^4 , which is block-diagonal and skew-symmetric:

$$J := J_1 \oplus J_2, \quad J_1 = J_2 := \begin{pmatrix} 0 & 1 \\ -1 & 0 \end{pmatrix}. \quad (3.5)$$

Any *bona fide* CM \mathcal{V} fulfills the concise Robertson-Schrödinger uncertainty relation:

$$\zeta^\dagger \left(\mathcal{V} + \frac{i}{2} J \right) \zeta \geq 0, \quad (\zeta \in \mathbb{C}^4). \quad (3.6)$$

Briefly stated, the matrix $\mathcal{V} + \frac{i}{2} J$ has to be positive semidefinite: $\mathcal{V} + \frac{i}{2} J \geq 0$. This requirement is a necessary and sufficient condition for the very existence of the Gaussian quantum state $\hat{\rho}$ [24–26]. It implies the inequality $\det(\mathcal{V} + \frac{i}{2} J) \geq 0$ and, in addition, that the CM \mathcal{V} is positive definite: $\mathcal{V} > 0$. The limit property $\det(\mathcal{V} + \frac{i}{2} J) = 0$ is therefore quite special. However, it is shared by all the pure GSs, as well by some interesting mixed ones. All these states are said to be at the physicality edge.

In the paper [8] we derived an explicit expression of the fidelity between a pair of two-mode GSs, $\hat{\rho}'$ and $\hat{\rho}''$, with the mean quadratures $v' := \langle \hat{u} \rangle_{\hat{\rho}'}$ and $v'' := \langle \hat{u} \rangle_{\hat{\rho}''}$, and the CMs \mathcal{V}' and \mathcal{V}'' , respectively. Let us denote their relative average displacement $\delta v := v' - v''$. We have found it convenient to employ three determinants satisfying the following inequalities:

$$\Delta := \det(\mathcal{V}' + \mathcal{V}'') \geq 1; \quad (3.7)$$

$$\Gamma := 2^4 \det \left[(J\mathcal{V}') (J\mathcal{V}'') - \frac{1}{4} I \right] \geq \Delta; \quad (3.8)$$

$$\Lambda := 2^4 \det \left(\mathcal{V}' + \frac{i}{2} J \right) \det \left(\mathcal{V}'' + \frac{i}{2} J \right) \geq 0. \quad (3.9)$$

In Eq. (3.8), I denotes the 4×4 identity matrix. The above determinants are manifestly symmetric with respect to the states $\hat{\rho}'$ and $\hat{\rho}''$ and so are the exact expressions of their overlap,

$$\text{Tr}(\hat{\rho}' \hat{\rho}'') = \frac{1}{\sqrt{\Delta}} \exp \left[-\frac{1}{2} (\delta v)^T (\mathcal{V}' + \mathcal{V}'')^{-1} \delta v \right] > 0, \quad (3.10)$$

and their fidelity [8],

$$\mathcal{F}(\hat{\rho}', \hat{\rho}'') = \left[\left(\sqrt{\Gamma} + \sqrt{\Lambda} \right) - \sqrt{\left(\sqrt{\Gamma} + \sqrt{\Lambda} \right)^2 - \Delta} \right]^{-1} \times \exp \left[-\frac{1}{2} (\delta v)^T (\mathcal{V}' + \mathcal{V}'')^{-1} \delta v \right]. \quad (3.11)$$

It is useful to introduce a pair of non-negative quantities:

$$K_{\pm} := \sqrt{\Gamma} + \sqrt{\Lambda} \pm \sqrt{\Delta}; \quad K_- \geq 0, \quad K_+ - K_- \geq 2. \quad (3.12)$$

The proportionality relation (A3) has the explicit form

$$\mathcal{F}(\hat{\rho}', \hat{\rho}'') = \left[1 + \sqrt{\frac{K_-}{\Delta}} \left(\sqrt{K_+} + \sqrt{K_-} \right) \right] \text{Tr}(\hat{\rho}' \hat{\rho}'') > 0, \quad (3.13)$$

which exhibits the general inequality (A4). The corresponding saturation condition,

$$\mathcal{F}(\hat{\rho}', \hat{\rho}'') = \text{Tr}(\hat{\rho}' \hat{\rho}'') \iff K_- = 0, \quad \text{i. e., } \Gamma = \Delta \text{ and } \Lambda = 0, \quad (3.14)$$

is partly redundant in comparison with the general conclusion (A6). Indeed, as shown in Appendix A, the latter equality, $\Lambda = 0$, is just a consequence of the former, $\Gamma = \Delta$.

We finally write down an alternative form of the fidelity (3.11) that we find appropriate to what follows:

$$\mathcal{F}(\hat{\rho}', \hat{\rho}'') = 2 \left(\sqrt{K_+} - \sqrt{K_-} \right)^{-2} \times \exp \left[-\frac{1}{2} (\delta v)^T (\mathcal{V}' + \mathcal{V}'')^{-1} \delta v \right]. \quad (3.15)$$

IV. SPECIAL TWO-MODE GAUSSIAN STATES

We focus on two important families of two-mode GSs that are obtained by employing simple optical instruments such as beam splitters and non-degenerate parametric down-converters. Two input light modes interact with the device and their coupling results in two output modes [27]. When the incoming beams are chosen to be in TSs, the outgoing ones are in a two-mode undisplaced GS. In a lossless beam splitter, a linear interaction mixes the incident waves to generate a MTS. By contrast, in a non-degenerate parametric amplifier, pumping of photons produces a non-linear interaction whose outcome is a STS.

Let us summarize the features of preparation and then recall a concise characterization of the above output states.

1. Each incident light wave is in a single-mode TS, so that the global input is their product, i.e., a two-mode TS on the Hilbert space $\mathcal{H}_1 \otimes \mathcal{H}_2$:

$$\begin{aligned} \hat{\rho}_T(\bar{n}_1, \bar{n}_2) &:= (\hat{\rho}_T)_1(\bar{n}_1) \otimes (\hat{\rho}_T)_2(\bar{n}_2) : \\ (\hat{\rho}_T)_j(\bar{n}_j) &:= \frac{1}{\bar{n}_j + 1} \exp\left(-\eta_j \hat{a}_j^\dagger \hat{a}_j\right), \\ (j = 1, 2), \end{aligned} \quad (4.1)$$

with $\hat{a}_j := \frac{1}{\sqrt{2}}(\hat{q}_j + i\hat{p}_j)$ denoting the photon annihilation operator of the mode j . In Eq. (4.1), \bar{n}_j is the Bose-Einstein mean photon number in the mode j ,

$$\bar{n}_j = [\exp(\eta_j) - 1]^{-1}, \quad (4.2)$$

and η_j is the positive dimensionless ratio

$$\eta_j := \frac{\hbar\omega_j}{k_B T_j} = \ln\left(\frac{\bar{n}_j + 1}{\bar{n}_j}\right). \quad (4.3)$$

2. The final effect of the mode coupling in both optical devices is modeled by a specific unitary operator that induces a linear transformation of the amplitude operators of the modes.
3. It is well known [28] that any two-mode GS $\hat{\rho}$ is similar, via a local unitary, to another one whose CM has a unique standard form which consists of a partitioning (3.4) into special diagonal 2×2 submatrices:

$$\begin{aligned} \mathcal{V}_j &= b_j \sigma_0, \quad \left(b_j \geq \frac{1}{2}\right), \quad (j = 1, 2), \\ \mathcal{C} &= \begin{pmatrix} c & 0 \\ 0 & d \end{pmatrix}, \quad (c \geq |d| \geq 0). \end{aligned} \quad (4.4)$$

In Eq. (4.4) and further on, σ_0 designates the 2×2 identity matrix. The four numbers b_1, b_2, c , and d are called the standard-form parameters of the given two-mode GS $\hat{\rho}$. However, there are special classes of two-mode GSs with a smaller number of such independent parameters. In particular, for TSs, $c = d = 0$, while for MTSS, $c = d > 0$, and for STSS, $c = -d > 0$.

A. Mode-mixed thermal states

The optical interference of two modes in a reversible, lossless beam splitter is described by a mode-mixing operator [29]:

$$\hat{M}_{12}(\theta, \phi) := \exp\left[\frac{\theta}{2}\left(e^{i\phi}\hat{a}_1\hat{a}_2^\dagger - e^{-i\phi}\hat{a}_1^\dagger\hat{a}_2\right)\right]. \quad (4.5)$$

Its parameters are the spherical polar angles θ and ϕ : $\theta \in [0, \pi]$, $\phi \in (-\pi, \pi]$. The co-latitude θ determines the

intensity transmission and reflection coefficients of the device, which are $T = [\cos(\frac{\theta}{2})]^2$ and $R = [\sin(\frac{\theta}{2})]^2$, respectively. The longitude ϕ accounts for a phase shifting. As a matter of fact, in view of the Jordan-Schwinger two-mode bosonic realization of angular momentum [30, 31],

$$\hat{J}_+ = \hat{a}_1^\dagger \hat{a}_2, \quad \hat{J}_- = \hat{a}_1 \hat{a}_2^\dagger, \quad \hat{J}_3 = \frac{1}{2}(\hat{a}_1^\dagger \hat{a}_1 - \hat{a}_2^\dagger \hat{a}_2), \quad (4.6)$$

the unitary operator (4.5) is a $SU(2)$ displacement operator [32, 33],

$$\hat{D}(\eta) := \exp\left(\eta \hat{J}_- - \eta^* \hat{J}_+\right), \quad \left(\eta := \frac{\theta}{2} e^{i\phi}\right), \quad (4.7)$$

acting on the two-mode Fock space $\mathcal{H}_1 \otimes \mathcal{H}_2$. At the same time, we employ the Euler angle parametrization to write it as a $SU(2)$ unitary representation operator whose carrier Hilbert space is $\mathcal{H}_1 \otimes \mathcal{H}_2$:

$$\begin{aligned} \hat{M}_{12}(\theta, \phi) &= \hat{\mathcal{D}}[U(\phi, \theta, -\phi)] \\ &= \exp\left(-i\phi \hat{J}_3\right) \exp\left(-i\theta \hat{J}_2\right) \exp\left(i\phi \hat{J}_3\right). \end{aligned} \quad (4.8)$$

When choosing an asymmetrical two-mode TS as input to the beam splitter, then we get an emerging MTS as its output:

$$\hat{\rho}_{MT} = \hat{M}_{12}(\theta, \phi) \hat{\rho}_T(\bar{n}_1, \bar{n}_2) \hat{M}_{12}^\dagger(\theta, \phi), \quad (\bar{n}_1 > \bar{n}_2). \quad (4.9)$$

To the unitary state evolution (4.9) in the Schrödinger picture is associated the $SU(2)$ matrix $U(\phi, \theta, -\phi)$ that transforms the annihilation operators in the Heisenberg picture,

$$\begin{pmatrix} \hat{a}'_1 \\ \hat{a}'_2 \end{pmatrix} = U(\phi, \theta, -\phi) \begin{pmatrix} \hat{a}_1 \\ \hat{a}_2 \end{pmatrix} :$$

$$U(\phi, \theta, -\phi) = \begin{pmatrix} \cos(\frac{\theta}{2}) & -\sin(\frac{\theta}{2}) e^{-i\phi} \\ \sin(\frac{\theta}{2}) e^{i\phi} & \cos(\frac{\theta}{2}) \end{pmatrix}. \quad (4.10)$$

In turn, the $SU(2)$ transformation (4.10) gives rise to a symplectic orthogonal one of the quadratures (3.1). Its matrix $S(\theta, \phi) \in Sp(4, \mathbb{R}) \cap O(4)$ has the following partition into 2×2 submatrices:

$$S(\theta, \phi) = \begin{pmatrix} \cos(\frac{\theta}{2}) \sigma_0 & -\sin(\frac{\theta}{2}) R(-\phi) \\ \sin(\frac{\theta}{2}) R(\phi) & \cos(\frac{\theta}{2}) \sigma_0 \end{pmatrix}. \quad (4.11)$$

We have employed the two-dimensional rotation matrix

$$R(\phi) := \begin{pmatrix} \cos(\phi) & -\sin(\phi) \\ \sin(\phi) & \cos(\phi) \end{pmatrix}, \quad (-\pi < \phi \leq \pi) :$$

$$R(\phi) = \cos(\phi) \sigma_0 - i \sin(\phi) \sigma_2, \quad (4.12)$$

where σ_2 is a Pauli matrix. In view of Eq. (B4), the CM of a two-mode TS (4.1) is diagonal:

$$\mathcal{V}_T(\bar{n}_1, \bar{n}_2) = \left(\bar{n}_1 + \frac{1}{2}\right) \sigma_0 \oplus \left(\bar{n}_2 + \frac{1}{2}\right) \sigma_0. \quad (4.13)$$

The unitary similarity (4.9) of the input and output two-mode GSs is equivalent to the symplectic congruence of their CMs:

$$\mathcal{V}_{MT}(\bar{n}_1, \bar{n}_2, \theta, \phi) = S(\theta, \phi) \mathcal{V}_T(\bar{n}_1, \bar{n}_2) S^T(\theta, \phi),$$

$$(\bar{n}_1 > \bar{n}_2). \quad (4.14)$$

Accordingly, the CM of the output MTS (4.9) has the 2×2 block structure

$$\mathcal{V}_{MT} = \begin{pmatrix} b_1 \sigma_0 & cR(-\phi) \\ cR(\phi) & b_2 \sigma_0 \end{pmatrix}, \quad (4.15)$$

with the standard-form entries:

$$b_1 = \left(\bar{n}_1 + \frac{1}{2}\right) \left[\cos\left(\frac{\theta}{2}\right)\right]^2 + \left(\bar{n}_2 + \frac{1}{2}\right) \left[\sin\left(\frac{\theta}{2}\right)\right]^2,$$

$$b_2 = \left(\bar{n}_1 + \frac{1}{2}\right) \left[\sin\left(\frac{\theta}{2}\right)\right]^2 + \left(\bar{n}_2 + \frac{1}{2}\right) \left[\cos\left(\frac{\theta}{2}\right)\right]^2,$$

$$c = d = (\bar{n}_1 - \bar{n}_2) \cos\left(\frac{\theta}{2}\right) \sin\left(\frac{\theta}{2}\right) > 0. \quad (4.16)$$

Needless to say, one gets the standard form (4.4) of the CM $\mathcal{V}_{MT}(\bar{n}_1, \bar{n}_2, \theta, \phi)$ of a MTS by setting $\phi = 0$ in Eq. (4.15). Note also that, in the limit case $\bar{n}_1 = \bar{n}_2 =: \bar{n}$, a two-mode MTS reduces to the input symmetric two-mode TS with the standard-form parameters

$$b_1 = b_2 =: b = \bar{n} + \frac{1}{2}, \quad c = 0. \quad (4.17)$$

This happens because the beam splitter has no influence upon two incident light beams whose one-mode states are identical.

B. Squeezed thermal states

The coupling of the modes in a non-degenerate parametric amplifier is modelled by the action of a two-mode squeeze operator [34],

$$\hat{S}_{12}(r, \phi) := \exp \left[r \left(e^{i\phi} \hat{a}_1^\dagger \hat{a}_2^\dagger - e^{-i\phi} \hat{a}_1 \hat{a}_2 \right) \right],$$

$$(r > 0, \quad \phi \in (-\pi, \pi]). \quad (4.18)$$

The positive dimensionless quantity r is called squeeze parameter [35]. Long ago, in a remarkable paper [36],

Yurke, McCall, and Klauder introduced a two-mode bosonic realization of the $su(1, 1)$ algebra:

$$\hat{K}_+ = \hat{a}_1^\dagger \hat{a}_2^\dagger, \quad \hat{K}_- = \hat{a}_1 \hat{a}_2,$$

$$\hat{K}_3 = \frac{1}{2} \left(\hat{a}_1^\dagger \hat{a}_1 + \hat{a}_2 \hat{a}_2^\dagger \right). \quad (4.19)$$

Starting from these formulae, a $SU(1, 1)$ unitary representation on the Hilbert space $\mathcal{H}_1 \otimes \mathcal{H}_2$ can be decomposed into irreducible unitary representations of $SU(1, 1)$ belonging to the positive discrete series [37]. Note that the Casimir operator

$$\hat{C} := -\hat{K}_+ \hat{K}_- - \hat{K}_3 + \hat{K}_3^2 \quad (4.20)$$

and the generator \hat{K}_3 are diagonal in the standard Fock basis of the Hilbert space $\mathcal{H}_1 \otimes \mathcal{H}_2$. Indeed, their eigenvalue equations have the solutions:

$$\hat{C} |k, m\rangle = k(k-1) |k, m\rangle, \quad \left(k = \frac{1}{2}, 1, \frac{3}{2}, 2, \frac{5}{2}, \dots\right),$$

$$\hat{K}_3 |k, m\rangle = m |k, m\rangle, \quad (m = k + l, \quad l = 0, 1, 2, 3, \dots):$$

$$|k, m\rangle_\pm := |\bar{n}_1, \bar{n}_2\rangle, \quad k := \frac{1}{2} (|\bar{n}_1 - \bar{n}_2| + 1),$$

$$m := \frac{1}{2} (\bar{n}_1 + \bar{n}_2 + 1), \quad |\bar{n}_1 - \bar{n}_2| = \pm (\bar{n}_1 - \bar{n}_2). \quad (4.21)$$

The two-mode Fock space $\mathcal{H}_1 \otimes \mathcal{H}_2$ is therefore an orthogonal sum of infinite-dimensional invariant subspaces which are labelled with the Bargmann index k :

$$\mathcal{H}_1 \otimes \mathcal{H}_2 = \mathcal{H}^{+(\frac{1}{2})} \oplus \bigoplus_{k > \frac{1}{2}} \left[\mathcal{H}_+^{+(k)} \oplus \mathcal{H}_-^{+(k)} \right]. \quad (4.22)$$

This property enables us to write the above-mentioned decomposition of a unitary representation of $SU(1, 1)$:

$$\hat{\mathcal{D}}(V) = \hat{\mathcal{D}}^{+(\frac{1}{2})}(V) \oplus \bigoplus_{k > \frac{1}{2}} \left[\hat{\mathcal{D}}^{+(k)}(V) \oplus \hat{\mathcal{D}}^{+(k)}(V) \right],$$

$$[V \in SU(1, 1)]. \quad (4.23)$$

Analogously to $SU(2)$, the corresponding $SU(1, 1)$ displacement operator acting on the Hilbert space $\mathcal{H}_1 \otimes \mathcal{H}_2$ [38, 39],

$$\hat{D}^+(\zeta) := \exp \left(\zeta \hat{K}_+ - \zeta^* \hat{K}_- \right),$$

$$\left(\zeta := \frac{\tau}{2} e^{i\phi}, \quad \tau \geq 0, \quad -\pi < \phi \leq \pi \right), \quad (4.24)$$

is a $SU(1, 1)$ unitary representation operator as well:

$$\hat{D}^+(\zeta) := \hat{\mathcal{D}}[V(\chi, \tau, -\chi)]$$

$$= \exp \left(-i\chi \hat{K}_3 \right) \exp \left(-i\tau \hat{K}_2 \right) \exp \left(i\chi \hat{K}_3 \right),$$

$$(\chi := -\phi \pm \pi : \quad -\pi < \chi \leq \pi). \quad (4.25)$$

Owing to the formulae (4.19), any two-mode squeeze operator (4.18) is at the same time a $SU(1,1)$ displacement operator (4.24) with the positive parameter $\tau = 2r$:

$$\hat{S}_{12}(r, \phi) = \hat{D}^+(r e^{i\phi}). \quad (4.26)$$

When the input to a non-degenerate parametric amplifier is a two-mode thermal radiation at optical frequencies, then its output is light in a STS:

$$\hat{\rho}_{\text{ST}} = \hat{S}_{12}(r, \phi) \hat{\rho}_{\text{T}}(\bar{n}_1, \bar{n}_2) \hat{S}_{12}^\dagger(r, \phi). \quad (4.27)$$

The unitary transformation (4.27) of the state in the Schrödinger picture determines the $SU(1,1)$ matrix $V(\chi, 2r, -\chi)$ corresponding to a Bogoliubov transformation of the amplitude operators in the Heisenberg picture:

$$\begin{pmatrix} \hat{a}'_1 \\ (\hat{a}'_2)^\dagger \end{pmatrix} = V(\chi, 2r, -\chi) \begin{pmatrix} \hat{a}_1 \\ \hat{a}_2^\dagger \end{pmatrix} :$$

$$V(\chi, 2r, -\chi) = \begin{pmatrix} \cosh(r) & \sinh(r) e^{i\phi} \\ \sinh(r) e^{-i\phi} & \cosh(r) \end{pmatrix}. \quad (4.28)$$

Further, the Bogoliubov transformation (4.28) is equivalent to a symplectic one of the quadratures (3.1). Its matrix $S(r, \phi) \in Sp(4, \mathbb{R})$ has the following 2×2 blocks expressed in terms of the identity and Pauli matrices:

$$S(r, \phi) = \begin{pmatrix} S_a & S_b \\ S_b & S_a \end{pmatrix} : \quad S_a := \cosh(r) \sigma_0,$$

$$S_b := \sinh(r) [\cos(\phi) \sigma_3 + \sin(\phi) \sigma_1]. \quad (4.29)$$

This symmetric matrix accomplishes a symplectic congruence of the type (4.14),

$$\mathcal{V}_{\text{ST}}(\bar{n}_1, \bar{n}_2, r, \phi) = S(r, \phi) \mathcal{V}_{\text{T}}(\bar{n}_1, \bar{n}_2) S^T(r, \phi). \quad (4.30)$$

We apply Eq. (4.30) to write the CM \mathcal{V}_{ST} of the output STS (4.27). This has the usual partition (3.4) with the symmetric 2×2 submatrices:

$$\mathcal{V}_j = b_j \sigma_0, \quad \left(b_j \geq \frac{1}{2} \right), \quad (j = 1, 2),$$

$$\mathcal{C} = c [\cos(\phi) \sigma_3 + \sin(\phi) \sigma_1], \quad (c > 0). \quad (4.31)$$

The standard form of the CM $\mathcal{V}_{\text{ST}}(\bar{n}_1, \bar{n}_2, r, \phi)$ of a STS is obtained by setting $\phi = 0$ in Eq. (4.31) and has the following parameters:

$$b_1 = \left(\bar{n}_1 + \frac{1}{2} \right) [\cosh(r)]^2 + \left(\bar{n}_2 + \frac{1}{2} \right) [\sinh(r)]^2,$$

$$b_2 = \left(\bar{n}_1 + \frac{1}{2} \right) [\sinh(r)]^2 + \left(\bar{n}_2 + \frac{1}{2} \right) [\cosh(r)]^2,$$

$$c = -d = (\bar{n}_1 + \bar{n}_2 + 1) \cosh(r) \sinh(r) > 0. \quad (4.32)$$

The only pure states belonging to the class of the STSs are the two-mode squeezed vacuum states (SVSs). Such a state is the output of a non-degenerate parametric amplifier when there is no photon at its input ports, that is, when both incoming field modes are in the vacuum state:

$$\hat{\rho}_{\text{SV}} = |\Psi_{\text{SV}}\rangle \langle \Psi_{\text{SV}}| : \quad |\Psi_{\text{SV}}\rangle = \hat{S}_{12}(r, \phi) |0, 0\rangle. \quad (4.33)$$

Note that the two-mode SVSs make up a two-parameter family of pure symmetric STSs, $(\bar{n}_1 = 0, \bar{n}_2 = 0)$, with the standard-form parameters:

$$b_1 = b_2 =: b = \frac{1}{2} \cosh(2r), \quad c = \frac{1}{2} \sinh(2r). \quad (4.34)$$

We finally mention that a comprehensive study of the transformation of the two-mode GSs in a non-degenerate parametric amplifier, including a detailed analysis of the conditions of separability and classicality of the output state, was carried out in an earlier paper [40]. Quite recently, we employed the sets of two-mode MTSs and STSs in a comparative investigation of the Hellinger distance as a Gaussian measure of all the correlations between the modes [18].

V. FIDELITY BETWEEN SPECIAL TWO-MODE GAUSSIAN STATES

We consider a pair of special two-mode GSs of the same kind, $\hat{\rho}'$ and $\hat{\rho}''$. Being undisplaced, the states are determined, respectively, by their CMs, \mathcal{V}' and \mathcal{V}'' , whose standard-form parameters are denoted $\{b'_1, b'_2, c'\}$ and $\{b''_1, b''_2, c''\}$. At the same time, their fidelity (3.15) has a simpler form:

$$\mathcal{F}(\hat{\rho}', \hat{\rho}'') = 2 \left(\sqrt{K_+} - \sqrt{K_-} \right)^{-2}. \quad (5.1)$$

A. Mode-mixed thermal states

Let $\{\bar{n}'_1, \bar{n}'_2, \theta', \phi'\}$ and $\{\bar{n}''_1, \bar{n}''_2, \theta'', \phi''\}$ stand for the parameters of the MTSs $\hat{\rho}'$ and $\hat{\rho}''$, respectively. Making use of the CM (4.15), we have evaluated the determinants Δ , Eq. (3.7) and Γ , Eq. (3.8), via the partitions of the corresponding 4×4 matrices into 2×2 blocks. We have applied the Schur determinant factorization (as the product of the determinant of a 2×2 principal submatrix by that of its Schur complement) to obtain the formulae:

$$\Delta = \{(b'_1 + b''_1)(b'_2 + b''_2) - [(c')^2 + (c'')^2 + 2c'c'' \cos(\phi' - \phi'')]\}^2; \quad (5.2)$$

$$\Gamma = 16 \left\{ [b'_1 b'_2 - (c')^2] [b''_1 b''_2 - (c'')^2] + \frac{1}{4} [b'_1 b''_1 + b'_2 b''_2 + 2c'c'' \cos(\phi' - \phi'')] + \frac{1}{16} \right\}^2. \quad (5.3)$$

The determinant Λ is the product (3.9) of two similar symplectic invariants:

$$\begin{aligned} \Lambda &= 16 \left\{ \left[b'_1 b'_2 - (c')^2 \right]^2 \right. \\ &\quad \left. - \frac{1}{4} \left[(b'_1)^2 + (b'_2)^2 + 2(c')^2 \right] + \frac{1}{16} \right\} \left\{ \left[b''_1 b''_2 - (c'')^2 \right]^2 \right. \\ &\quad \left. - \frac{1}{4} \left[(b''_1)^2 + (b''_2)^2 + 2(c'')^2 \right] + \frac{1}{16} \right\}. \end{aligned} \quad (5.4)$$

In the resulting functions K_{\pm} , Eq. (3.12), we substitute the specific expressions (4.16) of the standard-form parameters and get the following couple of formulae:

$$\begin{aligned} K_+ &= 2 \left\{ (\bar{n}'_1 \bar{n}'_2 \bar{n}''_1 \bar{n}''_2)^{\frac{1}{2}} \right. \\ &\quad \left. + [(\bar{n}'_1 + 1)(\bar{n}'_2 + 1)(\bar{n}''_1 + 1)(\bar{n}''_2 + 1)]^{\frac{1}{2}} \right\}^2. \end{aligned} \quad (5.5)$$

$$\begin{aligned} K_- &= 2 \left\{ [\bar{n}'_1 (\bar{n}'_2 + 1) \bar{n}''_1 (\bar{n}''_2 + 1)]^{\frac{1}{2}} \right. \\ &\quad \left. + [(\bar{n}'_1 + 1) \bar{n}'_2 (\bar{n}''_1 + 1) \bar{n}''_2]^{\frac{1}{2}} \right\}^2 \\ &\quad - (\bar{n}'_1 - \bar{n}'_2) (\bar{n}''_1 - \bar{n}''_2) \{1 - \cos(\theta' - \theta'')\} \\ &\quad + \sin(\theta') \sin(\theta'') [1 - \cos(\phi' - \phi'')]. \end{aligned} \quad (5.6)$$

Insertion of Eqs. (5.5) and (5.6) into Eq. (5.1) gives the fidelity of two MTSS. When all the other parameters of both states are kept fixed, this fidelity is an even function of the phase difference $\phi' - \phi''$, which is strictly decreasing in the interval $[0, \pi]$.

B. Squeezed thermal states

We focus on a pair of STSS, $\hat{\rho}'$ and $\hat{\rho}''$, and designate their sets of parameters as $\{\bar{n}'_1, \bar{n}'_2, r', \phi'\}$ and, respectively, $\{\bar{n}''_1, \bar{n}''_2, r'', \phi''\}$. Starting from the CM $\mathcal{V}_{\text{ST}}(\bar{n}_1, \bar{n}_2, r, \phi)$, specified by Eqs. (3.4) and (4.31), and employing the same technique as for MTSS, we have evaluated the determinants (3.7)- (3.9):

$$\begin{aligned} \Delta &= \{(b'_1 + b''_1)(b'_2 + b''_2) \\ &\quad - [(c')^2 + (c'')^2 + 2c'c'' \cos(\phi' - \phi'')]\}^2; \end{aligned} \quad (5.7)$$

$$\begin{aligned} \Gamma &= 16 \left\{ \left[b'_1 b'_2 - (c')^2 \right] \left[b''_1 b''_2 - (c'')^2 \right] \right. \\ &\quad \left. + \frac{1}{4} [b'_1 b''_1 + b'_2 b''_2 - 2c'c'' \cos(\phi' - \phi'')] + \frac{1}{16} \right\}^2; \end{aligned} \quad (5.8)$$

$$\begin{aligned} \Lambda &= 16 \left\{ \left[b'_1 b'_2 - (c')^2 \right]^2 - \frac{1}{4} \left[(b'_1)^2 + (b'_2)^2 - 2(c')^2 \right] + \frac{1}{16} \right\} \\ &\quad \times \left\{ \left[b''_1 b''_2 - (c'')^2 \right]^2 - \frac{1}{4} \left[(b''_1)^2 + (b''_2)^2 - 2(c'')^2 \right] + \frac{1}{16} \right\}. \end{aligned} \quad (5.9)$$

Substitution of the above formulae into Eq. (3.12) and subsequent insertion of the specific standard-form parameters (4.32) yield the following functions:

$$\begin{aligned} K_+ &= 2 \left\{ [\bar{n}'_1 \bar{n}'_2 (\bar{n}''_1 + 1) (\bar{n}''_2 + 1)]^{\frac{1}{2}} \right. \\ &\quad \left. + [(\bar{n}'_1 + 1) (\bar{n}'_2 + 1) \bar{n}''_1 \bar{n}''_2]^{\frac{1}{2}} \right\}^2 \\ &\quad + (\bar{n}'_1 + \bar{n}'_2 + 1) (\bar{n}''_1 + \bar{n}''_2 + 1) \{1 + \cosh[2(r' - r'')] \\ &\quad + \sinh(2r') \sinh(2r'') [1 - \cos(\phi' - \phi'')]\}. \end{aligned} \quad (5.10)$$

$$\begin{aligned} K_- &= 2 \left\{ [\bar{n}'_1 (\bar{n}'_2 + 1) \bar{n}''_1 (\bar{n}''_2 + 1)]^{\frac{1}{2}} \right. \\ &\quad \left. + [(\bar{n}'_1 + 1) \bar{n}'_2 (\bar{n}''_1 + 1) \bar{n}''_2]^{\frac{1}{2}} \right\}^2. \end{aligned} \quad (5.11)$$

By introducing the functions (5.10) and (5.11) into Eq. (5.1), we recover the expression of the fidelity between two STSS that has previously been used to quantify the Gaussian entanglement of such a two-mode state [41]. Concerning its dependence on the phase difference $\phi' - \phi''$, the fidelity between two STSS is an even function of this variable and strictly decreases with it in the interval $[0, \pi]$.

VI. QUANTUM FISHER INFORMATION TENSOR ON THE MANIFOLDS OF SPECIAL TWO-MODE GAUSSIAN STATES

Let us look at a quantum system which has a manifold of states that are characterized by a finite set of continuous real variables $\{\xi\}$. We concentrate on a pair of neighbouring states, $\hat{\rho}(\xi)$ and $\hat{\rho}(\xi + t d\xi)$, where t is a real non-negative variable. We apply Eq. (2.5):

$$\begin{aligned} \frac{1}{2} \{D_{\text{B}}[\hat{\rho}(\xi), \hat{\rho}(\xi + t d\xi)]\}^2 &= 1 - \sqrt{\mathcal{F}(t)}: \\ \mathcal{F}(t) &:= \mathcal{F}[\hat{\rho}(\xi), \hat{\rho}(\xi + t d\xi)], \quad (t \geq 0), \end{aligned} \quad (6.1)$$

Note the general properties:

$$\mathcal{F}(0) = 1, \quad - \left[\frac{d}{dt} \sqrt{\mathcal{F}(t)} \right]_{t=0} = 0. \quad (6.2)$$

The former identity in Eq. (6.2) represents the sufficiency part of the saturation case in Eq. (2.9), while the latter was proven by Hübner in Ref. [20]. Therefore, the first non-vanishing term in the Maclaurin series of the squared Bures distance (6.1) is the t^2 term:

$$\{D_{\text{B}}[\hat{\rho}(\xi), \hat{\rho}(\xi + t d\xi)]\}^2 = t^2 (d_{\text{SB}})^2 + \mathcal{O}(t^3). \quad (6.3)$$

Its coefficient is the squared infinitesimal Bures line element on the above-specified manifold,

$$(d_{\text{SB}})^2 = \sum_{\alpha} \sum_{\beta} g_{\alpha\beta}(\xi) d\xi_{\alpha} d\xi_{\beta}, \quad (6.4)$$

where $g_{\alpha\beta}(\xi)$ are the components of the affiliated Riemannian metric tensor. We will evaluate it for two-mode MTSS and STSS as the second-order derivative

$$(ds_B)^2 = - \left[\frac{d^2}{dt^2} \sqrt{\mathcal{F}(t)} \right]_{t=0} \geq 0. \quad (6.5)$$

In the realm of the GSs, this method was first applied by Twamley to evaluate the Bures geodesic metric for one-mode STSS [42]. Then it was used to evaluating and studying the QFI metric for single-mode displaced TSs [43] and quite recently for arbitrary one-mode GSs [44]. Here we take advantage of the natural parametrizations for both families of two-mode states, MTSS and STSS, as well as of the convenient formulae for their fidelity established in Sec. V.

A. Mode-mixed thermal states

The fidelity (6.1) between neighbouring MTSSs,

$$\begin{aligned} \mathcal{F}(t) &:= \mathcal{F}[\hat{\rho}(\bar{n}_1, \bar{n}_2, \theta, \phi), \\ &\hat{\rho}(\bar{n}_1 + t d\bar{n}_1, \bar{n}_2 + t d\bar{n}_2, \theta + t d\theta, \phi + t d\phi), \\ &(t \geq 0)], \end{aligned} \quad (6.6)$$

has the expression (5.1),

$$\mathcal{F}(t) = 2 \left[\sqrt{K_+(t)} - \sqrt{K_-(t)} \right]^{-2}, \quad (6.7)$$

with the functions $K_{\pm}(t)$ obviously introduced in the manner of Eq. (6.6). Hence the Bures metric (6.5) for MTSSs reads:

$$(ds_B)^2 = -\sqrt{2} \left\{ \frac{d^2}{dt^2} \left[\sqrt{K_+(t)} - \sqrt{K_-(t)} \right]^{-1} \right\}_{t=0}. \quad (6.8)$$

One can readily check the identities (6.2), the first one being precisely the sufficient condition in Eq. (C6). A straightforward calculation then yields the formula:

$$\begin{aligned} [(ds_B)_{\text{MT}}]^2 &= \frac{1}{4} \left(\frac{1}{\bar{n}_1(\bar{n}_1+1)} (d\bar{n}_1)^2 + \frac{1}{\bar{n}_2(\bar{n}_2+1)} (d\bar{n}_2)^2 \right. \\ &\left. + \frac{(\bar{n}_1 - \bar{n}_2)^2}{2\bar{n}_1\bar{n}_2 + \bar{n}_1 + \bar{n}_2} \left\{ (d\theta)^2 + [\sin(\theta)]^2 (d\phi)^2 \right\} \right). \end{aligned} \quad (6.9)$$

We have thus checked that the differentiable manifold $\mathcal{M}(\bar{n}_1, \bar{n}_2, \theta, \phi)$ of the two-mode MTSSs equipped with the Bures metric (6.9) is a Riemannian one. Besides, its metric tensor has a diagonal matrix $g_{\text{MT}}(\bar{n}_1, \bar{n}_2, \theta, \phi)$. Because the first two terms in Eq. (6.9) are not influenced by the action of the beam splitter, they depend only on the input two-mode TS $\hat{\rho}_{\text{T}}(\bar{n}_1, \bar{n}_2)$. Their sum defines therefore the Bures metric on the two-dimensional manifold $\mathcal{M}(\bar{n}_1, \bar{n}_2)$ of the two-mode TSs (4.1):

$$\begin{aligned} [(ds_B)_{\text{T}}]^2 &= \frac{1}{4} \left[\frac{1}{\bar{n}_1(\bar{n}_1+1)} (d\bar{n}_1)^2 \right. \\ &\left. + \frac{1}{\bar{n}_2(\bar{n}_2+1)} (d\bar{n}_2)^2 \right], \end{aligned} \quad (6.10)$$

With the reparametrization $\sqrt{\bar{n}_j} := \sinh(x_j)$, ($j = 1, 2$), the metric (6.10) becomes an Euclidean flat one:

$$[(ds_B)_{\text{T}}]^2 = (dx_1)^2 + (dx_2)^2. \quad (6.11)$$

This means that the Riemannian manifold $\mathcal{M}(\bar{n}_1, \bar{n}_2)$ is locally isometric with the first quadrant \mathbb{R}_+^2 of the Euclidean plane. The last two terms in Eq. (6.9) originate in the interaction of the incoming thermal modes with the beam splitter resulting in the $SU(2)$ unitary state evolution (4.9). Their sum is proportional to the Euclidean round metric on the two-dimensional unit sphere S^2 :

$$(ds_{\theta,\phi})^2 = (d\theta)^2 + [\sin(\theta)]^2 (d\phi)^2. \quad (6.12)$$

In this line, S^2 can be viewed as a compact homogeneous space: $S^2 = SU(2)/U(1)$.

Owing to the general relation (2.19), Eq. (6.9) provides additionally the statistical distance

$$\begin{aligned} [(ds_F)_{\text{MT}}]^2 &= H_{\bar{n}_1} (d\bar{n}_1)^2 + H_{\bar{n}_2} (d\bar{n}_2)^2 \\ &+ H_{\theta} (d\theta)^2 + H_{\phi} (d\phi)^2. \end{aligned} \quad (6.13)$$

The components of the diagonal QFI metric tensor are independent of the phase ϕ :

$$\begin{aligned} H_{\bar{n}_1} &= \frac{1}{\bar{n}_1(\bar{n}_1+1)}, & H_{\bar{n}_2} &= \frac{1}{\bar{n}_2(\bar{n}_2+1)}, \\ H_{\theta} &= \frac{(\bar{n}_1 - \bar{n}_2)^2}{2\bar{n}_1\bar{n}_2 + \bar{n}_1 + \bar{n}_2}, \\ H_{\phi} &= \frac{(\bar{n}_1 - \bar{n}_2)^2 [\sin(\theta)]^2}{2\bar{n}_1\bar{n}_2 + \bar{n}_1 + \bar{n}_2}. \end{aligned} \quad (6.14)$$

Since the above QFI matrix is diagonal, the natural parameters $\{\bar{n}_1, \bar{n}_2, \theta, \phi\}$ of the MTSSs are said to be orthogonal. According to Eqs. (6.13) and (6.14), the quantum Cramér-Rao lower bound for the variance of such a state estimator ξ_{α} reads [54]:

$$(\Delta\xi_{\alpha})^2 \geq \frac{1}{\mathcal{N}H_{\xi_{\alpha}}}, \quad (\xi_{\alpha} = \bar{n}_1, \bar{n}_2, \theta, \phi), \quad (6.15)$$

where \mathcal{N} is the number of measurements.

To sum up, the Bures metric (6.9) has the structure:

$$\begin{aligned} [(ds_B)_{\text{MT}}]^2 &= [(ds_B)_{\text{T}}]^2 + [f_{\text{MT}}(\bar{n}_1, \bar{n}_2)]^2 (ds_{\theta,\phi})^2 : \\ f_{\text{MT}}(\bar{n}_1, \bar{n}_2) &:= \frac{1}{2} \sqrt{H_{\theta}}. \end{aligned} \quad (6.16)$$

In addition, let us write down the Bures-metric volume element on the Riemannian manifold of the two-mode MTSSs:

$$d\mathcal{V}_B := \sqrt{\det[g_{\text{MT}}(\bar{n}_1, \bar{n}_2, \theta, \phi)]} d\bar{n}_1 d\bar{n}_2 d\theta d\phi. \quad (6.17)$$

This volume element is an invariant quantity under any change of parametrization. Moreover, by virtue of the formula

$$\sqrt{\det[g_{\text{MT}}(\bar{n}_1, \bar{n}_2, \theta, \phi)]} = \frac{1}{16} \sqrt{H_{\bar{n}_1} H_{\bar{n}_2} H_{\theta} H_{\phi}}, \quad (6.18)$$

it is proportional to the square root of the determinant of the QFI matrix:

$$\begin{aligned} \mathcal{J}_{\text{MT}}(\bar{n}_1, \bar{n}_2, \theta) &:= \sqrt{H_{\bar{n}_1} H_{\bar{n}_2} H_\theta H_\phi} : \\ \mathcal{J}_{\text{MT}}(\bar{n}_1, \bar{n}_2, \theta) &= \frac{1}{\sqrt{\bar{n}_1(\bar{n}_1+1)\bar{n}_2(\bar{n}_2+1)}} \\ &\times \frac{(\bar{n}_1 - \bar{n}_2)^2 \sin(\theta)}{2\bar{n}_1\bar{n}_2 + \bar{n}_1 + \bar{n}_2}. \end{aligned} \quad (6.19)$$

The function (6.19) is called quantum Jeffreys' prior [45] due to its role in Bayesian statistical inference [46]. Indeed, by extension of Jeffreys' geometric rule [47], when properly normalized, it is a reliable *a priori* probability density on any compact part of the state manifold $\mathcal{M}(\bar{n}_1, \bar{n}_2, \theta, \phi)$.

B. Squeezed thermal states

The fidelity (6.1) between neighbouring STSs,

$$\begin{aligned} \mathcal{F}(t) &:= \mathcal{F}[\hat{\rho}(\bar{n}_1, \bar{n}_2, r, \phi), \\ &\hat{\rho}(\bar{n}_1 + t d\bar{n}_1, \bar{n}_2 + t d\bar{n}_2, r + t dr, \phi + t d\phi)], \\ &(t \geq 0), \end{aligned} \quad (6.20)$$

is given by the formula (6.7), where the functions $K_\pm(t)$ are consistent with Eq. (6.20). Accordingly, the Bures metric (6.5) for STSs has the expression (6.8). It is easy to recover the identities (6.2), the first one being included in Eq. (C12). We are subsequently lead to the formula:

$$\begin{aligned} [(ds_{\text{B}})_{\text{ST}}]^2 &= \frac{1}{4} \left(\frac{1}{\bar{n}_1(\bar{n}_1+1)} (d\bar{n}_1)^2 + \frac{1}{\bar{n}_2(\bar{n}_2+1)} (d\bar{n}_2)^2 \right. \\ &\left. + \frac{(\bar{n}_1 + \bar{n}_2 + 1)^2}{2\bar{n}_1\bar{n}_2 + \bar{n}_1 + \bar{n}_2 + 1} \left\{ [d(2r)]^2 + [\sinh(2r)]^2 (d\phi)^2 \right\} \right). \end{aligned} \quad (6.21)$$

Equation (6.21) actually defines the Bures metric on the Riemannian manifold $\mathcal{M}(\bar{n}_1, \bar{n}_2, 2r, \phi)$ of the two-mode STSs. Note that the associated metric tensor has a diagonal matrix $g_{\text{ST}}(\bar{n}_1, \bar{n}_2, 2r, \phi)$. The sum of the first two terms in the r. h. s. of Eq. (6.21) is the squared line element (6.10) on the manifold $\mathcal{M}(\bar{n}_1, \bar{n}_2)$ of the two-mode TSs (4.1). The interaction of the incident thermal modes with the non-degenerate parametric amplifier produces the $SU(1, 1)$ unitary state evolution (4.27). This is represented by the last two terms in the r. h. s. of Eq. (6.21). Remarkably, their sum is proportional to the Minkowski metric on the hyperboloid of two sheets $x^2 + y^2 - z^2 = -1$:

$$(ds_{\tau, \phi})^2 = (d\tau)^2 + [\sinh(\tau)]^2 (d\phi)^2 : \quad \tau = 2r. \quad (6.22)$$

The upper sheet $z > 0$ of the hyperboloid is a two-dimensional Riemannian manifold denoted H_{-1}^2 , which is a non-compact homogeneous space: $H_{-1}^2 = SU(1, 1)/U(1)$. At the same time, H_{-1}^2 is an analytic model of the hyperbolic plane H^2 [48, 49].

By reason of the general relation (2.19), Eq. (6.21) supplies the infinitesimal statistical distance

$$\begin{aligned} [(ds_{\text{F}})_{\text{ST}}]^2 &= H_{\bar{n}_1} (d\bar{n}_1)^2 + H_{\bar{n}_2} (d\bar{n}_2)^2 \\ &+ H_{2r} [d(2r)]^2 + H_\phi (d\phi)^2, \end{aligned} \quad (6.23)$$

whose QFI matrix is diagonal, with entries independent of the phase ϕ :

$$\begin{aligned} H_{\bar{n}_1} &= \frac{1}{\bar{n}_1(\bar{n}_1+1)}, & H_{\bar{n}_2} &= \frac{1}{\bar{n}_2(\bar{n}_2+1)}, \\ H_{2r} &= \frac{(\bar{n}_1 + \bar{n}_2 + 1)^2}{2\bar{n}_1\bar{n}_2 + \bar{n}_1 + \bar{n}_2 + 1}, \\ H_\phi &= \frac{(\bar{n}_1 + \bar{n}_2 + 1)^2 [\sinh(2r)]^2}{2\bar{n}_1\bar{n}_2 + \bar{n}_1 + \bar{n}_2 + 1}. \end{aligned} \quad (6.24)$$

This diagonal form of the QFI tensor shows that the natural parameters $\{\bar{n}_1, \bar{n}_2, 2r, \phi\}$ of the STSs are orthogonal. It allows one to write directly the quantum Cramér-Rao bound for the variance of any such a state estimator ξ_α [54]:

$$(\Delta\xi_\alpha)^2 \geq \frac{1}{\mathcal{N}H_{\xi_\alpha}}, \quad (\xi_\alpha = \bar{n}_1, \bar{n}_2, 2r, \phi). \quad (6.25)$$

In Eq. (6.25), \mathcal{N} denotes the number of the performed measurements.

To recapitulate, we point out that the Bures metric (6.21) has a decomposition similar to that shown by Eq. (6.16):

$$\begin{aligned} [(ds_{\text{B}})_{\text{ST}}]^2 &= [(ds_{\text{B}})_{\text{T}}]^2 + [f_{\text{ST}}(\bar{n}_1, \bar{n}_2)]^2 (ds_{2r, \phi})^2 : \\ f_{\text{ST}}(\bar{n}_1, \bar{n}_2) &:= \frac{1}{2} \sqrt{H_{2r}}. \end{aligned} \quad (6.26)$$

Besides, we indicate the Bures-metric volume element on the Riemannian manifold $\mathcal{M}(\bar{n}_1, \bar{n}_2, 2r, \phi)$ of the two-mode STSs:

$$d\mathcal{V}_{\text{B}} := \sqrt{\det [g_{\text{ST}}(\bar{n}_1, \bar{n}_2, 2r, \phi)]} d\bar{n}_1 d\bar{n}_2 d(2r) d\phi. \quad (6.27)$$

The formula

$$\sqrt{\det [g_{\text{ST}}(\bar{n}_1, \bar{n}_2, 2r, \phi)]} = \frac{1}{16} \sqrt{H_{\bar{n}_1} H_{\bar{n}_2} H_{2r} H_\phi} \quad (6.28)$$

demonstrates that the parametrization-invariant volume element (6.27) is proportional to the quantum Jeffreys' prior:

$$\mathcal{J}_{\text{ST}}(\bar{n}_1, \bar{n}_2, 2r) := \sqrt{H_{\bar{n}_1} H_{\bar{n}_2} H_{2r} H_\phi}. \quad (6.29)$$

We recall the separability threshold r_s for a two-mode STS, introduced in Ref. [40]:

$$\sinh(r_s) := \sqrt{\frac{\bar{n}_1 \bar{n}_2}{\bar{n}_1 + \bar{n}_2 + 1}}. \quad (6.30)$$

Noticeably, the quantum Jeffreys' prior (6.29) depends only on two variables, r_s and r :

$$\mathcal{J}_{\text{ST}}(2r_s, 2r) = \frac{4 \sinh(2r)}{\sinh(4r_s)}. \quad (6.31)$$

At a fixed value of the squeeze parameter r , the function (6.31) strictly decreases with the variable r_s from the limit $\mathcal{J}_{\text{ST}}(0, 2r) = +\infty$ to zero, for $r_s \rightarrow +\infty$. The starting limit is reached by any two-mode STS at the physicality edge ($r_s = 0$) and, in particular, by any two-mode SVS. The value at the separability threshold $\mathcal{J}_{\text{ST}}(2r_s, 2r_s) = 2 \operatorname{sech}(2r_s)$ is itself a decreasing function of the variable r_s .

C. Discussion

We stress that the explicit formula (3.11) for the fidelity of two-mode GSs allows one the evaluation of QFI for estimating various parameters via Eq. (6.5). This method has efficiently been exploited in some recent applications [50, 51]. For instance, the concept of interferometric power, introduced and evaluated in Ref. [50], reduces in the particular case of an STS to the QFI matrix element H_ϕ , Eq. (6.24). A productive research [52, 53] in relativistic quantum metrology is based on QFI obtained by using Eq. (3.11).

However, there are few cases when one could use an explicit expression of the Uhlmann fidelity to derive the QFI metric via Eq. (6.5). The most widespread approach to evaluating the QFI is based on a central quantity in parameter estimation theory, namely, the symmetric logarithmic derivative (SLD) [21, 54]. In particular, some important results have been obtained for GSs by employing the SLD-method. An interesting example is the optimal estimation of entanglement for two-mode symmetric STSs in Ref. [55]. The QFI for one-parameter estimation in the case of multi-mode Gaussian channels and states was recently derived [56–58]. The general result for an n -mode GS obtained in Refs. [57, 58] is a compact expression in terms of the CM, the displacement vector, and their first-order derivatives with respect to the estimated parameter.

In order to check on Eqs. (6.14) and (6.24), we apply the QFI formula from Ref. [58] together with all the necessary ingredients involved. Making use of the CMs (4.15) and (4.31), as well as of the corresponding symplectic matrices (4.11) and (4.29) that diagonalize them by congruence, a routine calculation allows us to retrieve the QFI matrices for both manifolds of two-mode MTSs and STSs. However, the key point is the knowledge of the diagonalizing symplectic transformations.

VII. SCALAR CURVATURES OF THE BURES METRIC ON THE MANIFOLDS OF SPECIAL TWO-MODE GAUSSIAN STATES

The scalar curvature is the simplest invariant derived from the metric of a Riemannian or pseudo-Riemannian manifold. This is a real function R defined on such a manifold \mathcal{M} which is determined *solely* by its intrinsic geometry. The value $R(p)$ at each point $p \in \mathcal{M}$ depends

on the local features of the metric.

We evaluate the scalar curvatures on the four-dimensional Riemannian manifolds of the two-mode MTSs and STSs starting from their Bures metric tensors. Such a calculation exploits standard formulae from Riemannian Geometry [59] and consists of the following compulsory steps:

1. Evaluation of the Christoffel symbols of the Levi-Civita connection;
2. Calculation of the required components of the Riemann curvature tensor by employing the Christoffel symbols and their first-order derivatives;
3. Calculation of the diagonal components of the Ricci tensor, which is defined as a contraction of the Riemann tensor;
4. Evaluation of the Riemannian scalar curvature as the trace of the Ricci tensor with respect to the metric.

We mention that calculations of the scalar curvature of the Bures metric tensor along the same lines were carried out previously for Riemannian manifolds of two kinds of single-mode GSs, namely, the STSs [42] and the displaced TSs [43].

A. Mode-mixed thermal states

By carrying out the above-sketched program, we have found the scalar curvature on the Riemannian manifold $\mathcal{M}(\bar{n}_1, \bar{n}_2, \theta, \phi)$ of the two-mode MTSs:

$$R_{\text{MT}}(\bar{n}_1, \bar{n}_2) = \frac{2}{(2\bar{n}_1\bar{n}_2 + \bar{n}_1 + \bar{n}_2)^2} \times \left[(\bar{n}_1 - \bar{n}_2)^2 - 24\bar{n}_1(\bar{n}_1 + 1)\bar{n}_2(\bar{n}_2 + 1) + 9(2\bar{n}_1\bar{n}_2 + \bar{n}_1 + \bar{n}_2) \right]. \quad (7.1)$$

The scalar curvature (7.1) does not depend on the parameters $\{\theta, \phi\}$ of the beam splitter. Its expression is valid for any values of the mean thermal photon occupancies \bar{n}_1, \bar{n}_2 , and displays the symmetry property

$$R_{\text{MT}}(\bar{n}_2, \bar{n}_1) = R_{\text{MT}}(\bar{n}_1, \bar{n}_2). \quad (7.2)$$

Therefore, Eq. (7.1) describes a two-dimensional surface in \mathbb{R}^3 which is represented in Fig. 1. It looks like a descending symmetric valley whose talweg is precisely the intersection with its symmetry plane $\bar{n}_1 = \bar{n}_2$, i.e., the vertical plane that bisects the first octant.

In the limit case $\bar{n}_1 = \bar{n}_2 =: \bar{n}$ of an emerging two-mode TS, Eq. (7.1) simplifies to:

$$R_{\text{MT}}(\bar{n}, \bar{n}) = \frac{9}{\bar{n}(\bar{n} + 1)} - 12. \quad (7.3)$$

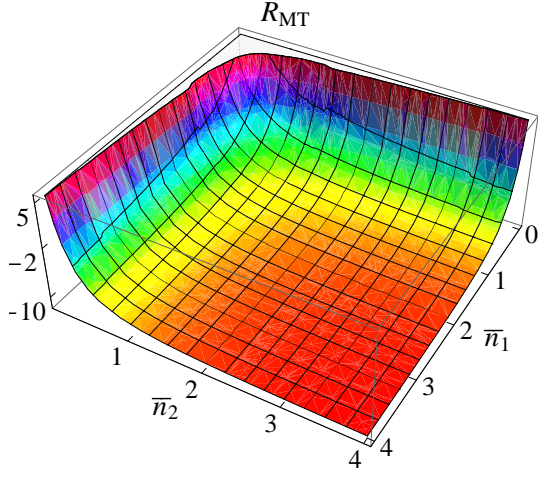


FIG. 1. (Color online) The scalar curvature $R_{\text{MT}}(\bar{n}_1, \bar{n}_2)$, Eq. (7.1), of the two-mode MTSs. This is a convex surface whose general aspect is that of a symmetric valley that descends and widens continuously. Its talweg belongs to the symmetry plane $\bar{n}_1 = \bar{n}_2$ and is drawn in Fig. 2a.

The graph of the above function is the intersection of the two-dimensional surface (7.1) and its symmetry plane $\bar{n}_1 = \bar{n}_2$. The function (7.3) strictly decreases with the variable \bar{n} from $+\infty$ at $\bar{n} = 0$ to the negative asymptotic value $\lim_{\bar{n} \rightarrow \infty} R_{\text{MT}}(\bar{n}, \bar{n}) = -12$. Besides, this is a convex function which has a unique zero, $\bar{n} = \frac{1}{2}$.

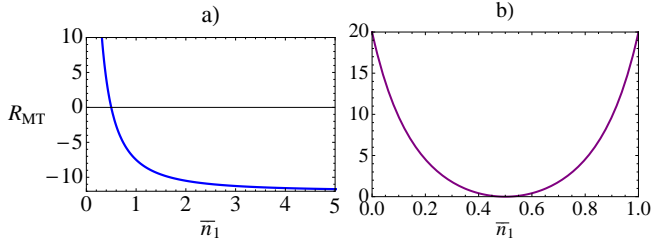


FIG. 2. (Color online) a) The vertical intersection (7.3) of the surface (7.1) and its symmetry plane $\bar{n}_1 = \bar{n}_2$. This is the talweg of the surface (7.1) and is made up of the symmetric two-mode TSs.

b) The vertical intersection (7.4) of the surface (7.1) and the plane $\bar{n}_1 + \bar{n}_2 = 1$. The vertical sections a) and b) which are orthogonal and meet at their unique zero, $\bar{n}_1 = \frac{1}{2}$.

It is instructive to examine further the intersection of the surface (7.1) and a vertical plane perpendicular to its symmetry plane. As an example, we choose the plane $\bar{n}_1 + \bar{n}_2 = 1$ which meets the symmetry plane in the vertical line $\bar{n}_1 = \bar{n}_2 = \frac{1}{2}$. This straight line contains the above-mentioned zero of the function (7.3). The intersection of the surface (7.1) and the vertical plane $\bar{n}_1 + \bar{n}_2 = 1$ is the graph of the following function of the

variable $\bar{n}_1 \in [0, 1]$:

$$R_{\text{MT}}(\bar{n}_1, 1 - \bar{n}_1) = -4 \frac{12\alpha^2 + 17\alpha - 5}{(2\alpha + 1)^2} \geq 0, \quad (7.4)$$

$$\alpha := \bar{n}_1(1 - \bar{n}_1) \in \left[0, \frac{1}{4}\right].$$

The function (7.4) strictly decreases from the limit value $R_{\text{MT}}(0, 1) = 20$ to its minimum $R_{\text{MT}}(\frac{1}{2}, \frac{1}{2}) = 0$ and then has a mirror increase on the interval $\bar{n}_1 \in [\frac{1}{2}, 1]$. Its graph exhibits the profile of a symmetric valley. Such a vertical section is typical for the two-dimensional surface (7.1). The vertical sections (7.3) and (7.4) are plotted in Figs. 2a and 2b.

A noteworthy limit situation arises when one incoming mode is in the vacuum state and the other is not ($\bar{n}_1 > 0$, $\bar{n}_2 = 0$). Then the output two-mode MTS is at the physicality edge and has the scalar curvature

$$R_{\text{MT}}(\bar{n}_1, 0) = 2 + \frac{18}{\bar{n}_1}. \quad (7.5)$$

The function (7.5) is positive, strictly decreasing and convex. Figure 5 presents its graph, as well as that of the function (7.10).

B. Squeezed thermal states

In a similar way we have evaluated the scalar curvature on the Riemannian manifold $\mathcal{M}(\bar{n}_1, \bar{n}_2, 2r, \phi)$ of the two-mode STSs:

$$R_{\text{ST}}(\bar{n}_1, \bar{n}_2) = \frac{2}{(2\bar{n}_1\bar{n}_2 + \bar{n}_1 + \bar{n}_2 + 1)^2} \times \left[(\bar{n}_1 + \bar{n}_2 + 1)^2 - 24\bar{n}_1(\bar{n}_1 + 1)\bar{n}_2(\bar{n}_2 + 1) - 9(2\bar{n}_1\bar{n}_2 + \bar{n}_1 + \bar{n}_2 + 1) \right]. \quad (7.6)$$

The scalar curvature (7.6) does not depend on the parameters $\{2r, \phi\}$ of the non-degenerate parametric amplifier. Its expression is valid for any values of the mean thermal photon occupancies \bar{n}_1, \bar{n}_2 , and displays the symmetry property

$$R_{\text{ST}}(\bar{n}_2, \bar{n}_1) = R_{\text{ST}}(\bar{n}_1, \bar{n}_2). \quad (7.7)$$

Accordingly, the two-dimensional surface (7.6) in \mathbb{R}^3 has the vertical symmetry plane $\bar{n}_1 = \bar{n}_2$ that bisects the first octant. Figure 3 displays the general aspect of this surface. It looks like a pair of opposite symmetric valleys. The ascending valley is narrow and steep, while the descending one is broader and slower. The talweg is the intersection (7.8) with the symmetry plane $\bar{n}_1 = \bar{n}_2$, while the watershed is the intersection (7.9) with the vertical plane $\bar{n}_1 + \bar{n}_2 = 2\bar{n}_s$, which is perpendicular to the first one. The talweg and the watershed are tangent at

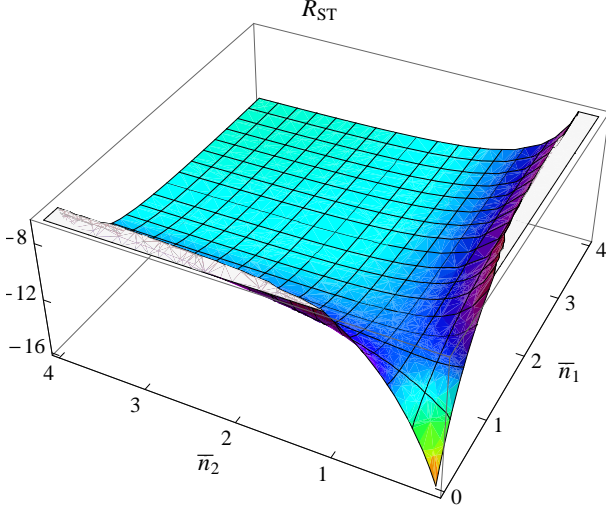


FIG. 3. (Color online) The scalar curvature $R_{ST}(\bar{n}_1, \bar{n}_2)$, Eq. (7.6), of the two-mode STSs. This surface consists of two opposite symmetric valleys separated by a watershed: a narrow, steeply ascending valley and a wider one which is slowly descending. It possesses a unique saddle point S at the intersection of the talweg and the watershed. The talweg is the normal section (7.8) in the symmetry plane $\bar{n}_1 = \bar{n}_2$, while the watershed is the normal section (7.9) in the plane $\bar{n}_1 + \bar{n}_2 = 2\bar{n}_s$. These normal sections, which are vertical and orthogonal, are represented in Figs. 4a and 4b.

the unique saddle point S on the surface, which is located at the point (\bar{n}_s, \bar{n}_s) with $\bar{n}_s := -0.5 + \sqrt{1.15} \approx 0.5724$.

For symmetric two-mode STSs, ($\bar{n}_1 = \bar{n}_2 =: \bar{n}$), the scalar curvature (7.6) is negative:

$$R_{ST}(\bar{n}, \bar{n}) = -4 \frac{12\beta^2 + 7\beta + 4}{(2\beta + 1)^2} < 0, \quad \beta := \bar{n}(\bar{n} + 1) \geq 0. \quad (7.8)$$

The graph of the above function is reproduced in Fig. 4a and is the talweg of the surface (7.6). On its ascending side, the function (7.8) has a steep rise from the limit value $R_{ST}(0, 0) = -16$, reached for any two-mode SVS, to a maximum $R_{ST}(\bar{n}_s, \bar{n}_s) = -\frac{143}{14} \approx -10.2143$, reached at the point $\bar{n}_s = -0.5 + \sqrt{1.15} \approx 0.5724$. Then, on the descending side, it has a moderate fall toward the asymptotic value $\lim_{\bar{n} \rightarrow \infty} R_{ST}(\bar{n}, \bar{n}) = -12$. As expected on intuitive grounds, this asymptotic limit coincides with the similar one for MTSs, displayed in Fig. 2a: $\lim_{\bar{n} \rightarrow \infty} R_{MT}(\bar{n}, \bar{n}) = -12$.

Let us contemplate next the intersection of the surface (7.6) and the vertical plane $\bar{n}_1 + \bar{n}_2 = 2\bar{n}_s$, where \bar{n}_s is the maximum point of the function (7.8). This plane is perpendicular to the symmetry plane $\bar{n}_1 = \bar{n}_2$ and meets it in the vertical straight line $\bar{n}_1 = \bar{n}_2 = \bar{n}_s$. The aforementioned intersection is the graph of the following

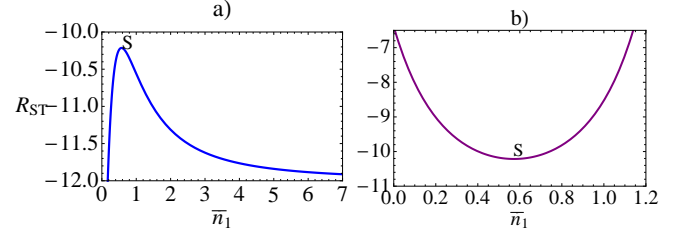


FIG. 4. (Color online) a) The vertical intersection (7.8) of the surface (7.6) and its symmetry plane $\bar{n}_1 = \bar{n}_2$. This is the talweg of the surface (7.6) and is made up of the symmetric two-mode STSs.

The function (7.8) has a steep rise from its lowest value $R_{ST}(0, 0) = -16$, reached for any two-mode SVS, to a maximum $R_{ST}(\bar{n}_s, \bar{n}_s) = -\frac{143}{14} \approx -10.2143$, reached at the point $\bar{n}_s = -0.5 + \sqrt{1.15} \approx 0.5724$. Then it has a moderate fall toward the asymptotic value $\lim_{\bar{n} \rightarrow \infty} R_{ST}(\bar{n}, \bar{n}) = -12$. The function (7.8) changes concavity at the unique inflection point $\bar{n}_i \approx 0.9565$, where it has the value $R_{ST}(\bar{n}_i, \bar{n}_i) \approx -10.5140$. b) The vertical intersection (7.9) of the surface (7.6) and the plane $\bar{n}_1 + \bar{n}_2 = 2\bar{n}_s$. This is the watershed on the surface (7.6), which is orthogonal to the talweg and touches it at their common extremum point, $\bar{n}_1 = \bar{n}_s$.

function of the variable $\bar{n}_1 \in [0, 2\bar{n}_s]$:

$$R_{ST}(\bar{n}_1, 2\bar{n}_s - \bar{n}_1) = -\frac{4}{[2(\gamma + \bar{n}_s) + 1]^2} \times [12(\gamma + \bar{n}_s)^2 + 21(\gamma + \bar{n}_s) - 8.6] < 0, \quad \gamma := \bar{n}_1(2\bar{n}_s - \bar{n}_1) \in [0, (\bar{n}_s)^2], \quad (\bar{n}_s)^2 = 0.3276, \quad 4 - 14\bar{n}_s(\bar{n}_s + 1) = 8.6. \quad (7.9)$$

The function (7.9) decreases from the limit value $R_{ST}(0, 2\bar{n}_s) \approx -6.3925$ to its minimum, $R_{ST}(\bar{n}_s, \bar{n}_s) = -\frac{143}{14} \approx -10.2143$, and then has a mirror increase on the interval $\bar{n}_1 \in [\bar{n}_s, 2\bar{n}_s]$. Its graph is therefore the profile of a symmetric valley and is drawn in Fig. 4b.

Although such a vertical section is typical for the two-dimensional surface (7.6), the section (7.9) is a rather special one. Indeed, the common extremum point $S : \{\bar{n}_s, \bar{n}_s, R_{ST}(\bar{n}_s, \bar{n}_s)\}$ of the curves (7.8) and (7.9) is a saddle point on the two-dimensional surface (7.6) in \mathbb{R}^3 , having an upward vertical normal. Moreover, this turns out to be its unique stationary point. The curves (7.8) and (7.9) are precisely the normal sections that include the principal directions tangent to the surface (7.6) at the saddle point S [60].

When one of the incoming modes is in the vacuum state and the other is not, ($\bar{n}_1 > 0, \bar{n}_2 = 0$), then the output two-mode STS is at the physicality edge. It has the scalar curvature

$$R_{ST}(\bar{n}_1, 0) = 2 - \frac{18}{\bar{n}_1 + 1}. \quad (7.10)$$

The function (7.10) strictly increases with the variable \bar{n}_1 from the SVS value $R_{ST}(0, 0) = -16$ to the positive

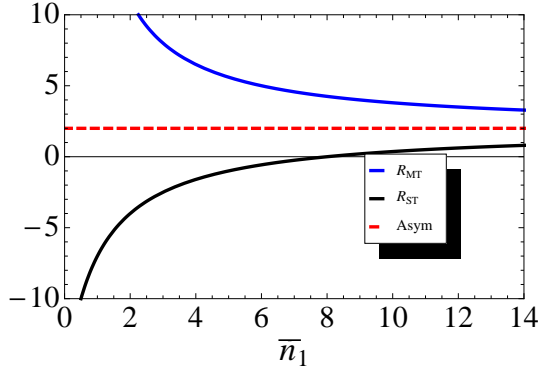


FIG. 5. (Color online) The scalar curvatures (7.5) and (7.10) of the two-mode MTSs and STSs at the physicality edge. They are figured as the marginal vertical curves on the surfaces (7.1) and (7.6), respectively, which meet the plane $\bar{n}_2 = 0$ along them. The former is decreasing and convex, while the latter is increasing and concave. Their starting values are, respectively, $R_{\text{MT}}(0, 0) = +\infty$ for the vacuum state and $R_{\text{ST}}(0, 0) = -16$ for any two-mode SVS. Nevertheless, they have a common asymptotic limit: $R_{\text{MT}}(+\infty, 0) = R_{\text{ST}}(+\infty, 0) = 2$.

asymptotic value $\lim_{\bar{n}_1 \rightarrow \infty} R_{\text{ST}}(\bar{n}_1, 0) = 2$. Besides, it is a concave function which has a unique zero, $\bar{n}_1 = 8$. The curves (7.5) and (7.10) have a common asymptote and are represented together in Fig. 5.

C. Alternative derivation

The most intriguing feature of both scalar curvatures $R_{\text{MT}}(\bar{n}_1, \bar{n}_2)$, Eq. (7.1), and $R_{\text{ST}}(\bar{n}_1, \bar{n}_2)$, Eq. (7.6), is that they do not depend on the parameters $\{\theta, \phi\}$ and, respectively, $\{2r, \phi\}$. These parameters specify the unitary transformations modeling the interactions of the incident thermal-light beams with the optical devices under discussion. Nevertheless, the scalar curvatures originate precisely in the mentioned unitary transformations. Since the scalar curvature of a given metric on a Riemannian manifold is determined solely by the metric itself, any explanation should start from the decompositions (6.16) and (6.26) of the squared Bures line elements on the Riemannian manifolds of special two-mode GSs. They can be written in terms of the metric tensors as follows:

$$g_{\text{MT}}(\bar{n}_1, \bar{n}_2, \theta, \phi) = g_{\text{T}}(\bar{n}_1, \bar{n}_2) \oplus [f_{\text{MT}}(\bar{n}_1, \bar{n}_2)]^2 g_{S^2}(\theta, \phi); \quad (7.11)$$

$$g_{\text{ST}}(\bar{n}_1, \bar{n}_2, 2r, \phi) = g_{\text{T}}(\bar{n}_1, \bar{n}_2) \oplus [f_{\text{ST}}(\bar{n}_1, \bar{n}_2)]^2 g_{H_{-1}^2}(2r, \phi). \quad (7.12)$$

In the above equations, g_{S^2} and $g_{H_{-1}^2}$ designate the metric tensors on the two-dimensional Riemannian manifolds

S^2 and H_{-1}^2 , as given by Eqs. (6.12) and (6.22), respectively. In contrast to the Euclidean plane, these surfaces have a constant scalar curvature which is not zero. Moreover, up to a scale factor, they are the only connected ones to share this intrinsic geometric property:

$$R(\mathbb{R}^2) = 0, \quad R(S^2) = 2, \quad R(H_{-1}^2) = -2. \quad (7.13)$$

We further need the notion of warped product of two Riemannian manifolds, which was introduced in Ref. [61]. Let $(\mathcal{B}, g_{\mathcal{B}})$ and $(\mathcal{F}, g_{\mathcal{F}})$ be Riemannian manifolds of dimensions m and n , respectively, and $f : \mathcal{B} \rightarrow \mathbb{R}_+ \setminus \{0\}$ a smooth function: $f \in C^\infty(\mathcal{B})$. The warped product $\mathcal{M} := \mathcal{B} \times_f \mathcal{F}$ is the differentiable product manifold $\mathcal{B} \times \mathcal{F}$, of dimension $m + n$, endowed with the Riemannian metric $g_{\mathcal{M}} := g_{\mathcal{B}} \oplus f^2 g_{\mathcal{F}}$. By means of this rule, the warping function $f > 0$ determines the Riemannian structure of the warped product $(\mathcal{M}, g_{\mathcal{M}})$.

The relationship between the scalar curvatures $R(\mathcal{B})$, $R(\mathcal{F})$, and $R(\mathcal{M})$ was established in Ref. [62]:

$$-\frac{4n}{n+1} \Delta_{g_{\mathcal{B}}} u + R(\mathcal{B})u + R(\mathcal{F})u^{\frac{n-3}{n+1}} = R(\mathcal{M})u, \quad (7.14)$$

$$u := f^{\frac{n+1}{2}}.$$

In Eq. (7.14), $\Delta_{g_{\mathcal{B}}}$ is the Laplace-Beltrami operator on the Riemannian manifold $(\mathcal{B}, g_{\mathcal{B}})$. This second-order differential operator is the divergence of the gradient:

$$\Delta_{g_{\mathcal{B}}} v = \frac{1}{\sqrt{\det(g_{\mathcal{B}})}} \partial_j \left[\sqrt{\det(g_{\mathcal{B}})} (g_{\mathcal{B}})^{jk} \partial_k v \right], \quad (7.15)$$

$$v \in C^2(\mathcal{B}).$$

We mention two important consequences of Eq. (7.14).

First, when $f = 1$, it reduces to the familiar addition law

$$R(\mathcal{B} \times \mathcal{F}) = R(\mathcal{B}) + R(\mathcal{F}) \quad (7.16)$$

for the scalar curvature of the Riemannian product manifold $(\mathcal{B} \times \mathcal{F}, g_{\mathcal{B}} \oplus g_{\mathcal{F}})$.

Second, the scalar curvature $R(\mathcal{M})$ of the warped product $\mathcal{M} := \mathcal{B} \times_f \mathcal{F}$ does not depend on the parameters of the manifold \mathcal{F} if and only if \mathcal{F} has a constant scalar curvature.

Coming back to our current problem, the structure of the metric tensors (7.11) and (7.12) shows that the four-dimensional Riemannian manifolds $\mathcal{M}(\bar{n}_1, \bar{n}_2, \theta, \phi)$ and $\mathcal{M}(\bar{n}_1, \bar{n}_2, 2r, \phi)$ are warped products:

$$\mathcal{M}(\bar{n}_1, \bar{n}_2, \theta, \phi) = \mathcal{M}(\bar{n}_1, \bar{n}_2) \times_{f_{\text{MT}}} S^2(\theta, \phi); \quad (7.17)$$

$$\mathcal{M}(\bar{n}_1, \bar{n}_2, 2r, \phi) = \mathcal{M}(\bar{n}_1, \bar{n}_2) \times_{f_{\text{ST}}} H_{-1}^2(2r, \phi). \quad (7.18)$$

In view of the isometry (6.11), the two-dimensional Riemannian manifold $\mathcal{M}(\bar{n}_1, \bar{n}_2) \equiv \mathbb{R}_+^2$ of the two-mode TSs (4.1) has a vanishing scalar curvature. However, the essential issue is that both S^2 and H_{-1}^2 are surfaces

of constant scalar curvature. Then the second consequence stated above explains why the scalar curvatures $R_{\text{MT}}(\bar{n}_1, \bar{n}_2)$ and $R_{\text{ST}}(\bar{n}_1, \bar{n}_2)$ depend only on the mean thermal photon numbers in the incoming modes. Needless to say, this dependence is specific for each of the warped products (7.17) and (7.18).

Let us check on our formulae (7.1) and (7.6) by specializing Eqs. (7.14) and (7.15) for the warped products (7.17) and (7.18), respectively. Taking account of Eqs. (6.14), (6.16), (6.24), (6.26), and (7.13), we find the following pair of equations for the scalar curvatures:

$$R_{\text{MT}}(\bar{n}_1, \bar{n}_2) = \frac{8}{H_\theta} - 2 \sum_{j=1}^2 \bar{n}_j (\bar{n}_j + 1) \left\{ 4 \frac{\partial^2}{\partial \bar{n}_j^2} \ln(H_\theta) + 3 \left[\frac{\partial}{\partial \bar{n}_j} \ln(H_\theta) \right]^2 \right\} - 4 \sum_{j=1}^2 (2\bar{n}_j + 1) \frac{\partial}{\partial \bar{n}_j} \ln(H_\theta),$$

$$(\bar{n}_1 \neq \bar{n}_2); \quad (7.19)$$

$$R_{\text{ST}}(\bar{n}_1, \bar{n}_2) = -\frac{8}{H_{2r}} - 2 \sum_{j=1}^2 \bar{n}_j (\bar{n}_j + 1) \left\{ 4 \frac{\partial^2}{\partial \bar{n}_j^2} \ln(H_{2r}) + 3 \left[\frac{\partial}{\partial \bar{n}_j} \ln(H_{2r}) \right]^2 \right\} - 4 \sum_{j=1}^2 (2\bar{n}_j + 1) \frac{\partial}{\partial \bar{n}_j} \ln(H_{2r}).$$

$$(7.20)$$

Substitution of the functions H_θ and H_{2r} into the above equations yields the expected formulae (7.1) and (7.6).

VIII. SUMMARY AND CONCLUSIONS

We start this overview by stressing the main results we have obtained in the present work. First, we have established an alternative expression of the fidelity between two-mode GSs, Eq. (3.15). On the one hand, this is efficient in evaluating the fidelity between special states, as it happens with the two-mode MTSs, Eqs. (5.5)- (5.6), and the two-mode STSs, Eqs. (5.10)- (5.11). On the other hand, it is flexible enough to have checked with ease, in Appendix C, the inequality $\mathcal{F}(\hat{\rho}', \hat{\rho}'') \leq 1$ for both families of special two-mode GSs.

Second, taking advantage of the above-cited formulae, we have derived the Bures infinitesimal geodesic distances on the Riemannian manifolds $\mathcal{M}(\bar{n}_1, \bar{n}_2, \theta, \phi)$ of the two-mode MTSs, Eq. (6.9), and $\mathcal{M}(\bar{n}_1, \bar{n}_2, 2r, \phi)$ of the two-mode STSs, Eq. (6.21). They are statistically relevant due to the proportionality between the Bures and QFI metric tensors [21]. This endows the Bures metric with the general feature of statistical distinguishability between neighbouring states on a Riemannian manifold when performing suitable quantum measurements. In addition, the diagonal form of the QFI metric tensors (6.14) of MTSs and (6.24) of STSs with respect to their natural parameters simplifies the corresponding quantum Cramér-Rao inequalities.

Third, we have employed a standard procedure to evaluate the scalar curvature associated to the Bures metric on each of the Riemannian manifolds $\mathcal{M}(\bar{n}_1, \bar{n}_2, \theta, \phi)$ of the two-mode MTSs and $\mathcal{M}(\bar{n}_1, \bar{n}_2, 2r, \phi)$ of the two-mode STSs. The formulae (7.1) and (7.6) are the corresponding exact analytic results. Both scalar curvatures are merely functions of the mean photon numbers in the incident thermal modes, \bar{n}_1 and \bar{n}_2 . In spite of being determined by the interaction of thermal radiation with the optical instruments described previously, neither of them depends on the specific parameters of the optical device involved. This particular property stems from the symmetry nature of the unitary operators (4.5) and (4.18) describing the optical processes in question: $SU(2)$ and, respectively, $SU(1,1)$. In addition, we have exploited these symmetries to recover the scalar curvatures (7.1) and (7.6) by an alternative method. Figures 1 and 3 allow one to visualize each of them as a function of the mean photon occupancies of the incoming thermal modes.

In order to reveal the significance of the Bures scalar curvature, we follow closely Petz's exposition in Ref. [63]. Let us consider an n -dimensional Riemannian manifold (\mathcal{M}, g_B) of quantum states, which is equipped with the Bures metric g_B . Then the geodesic distance $D_B(\hat{\rho}', \hat{\rho}'')$ between two points on the manifold \mathcal{M} is interpreted as the statistical distinguishability of the two states by means of the optimal quantum measurement.

We focus on a given state $\hat{\rho}_0 \in (\mathcal{M}, g_B)$. The geodesic ball

$$B_n(\hat{\rho}_0; \varepsilon) := \{\hat{\rho} \in (\mathcal{M}, g_B) : D_B(\hat{\rho}_0, \hat{\rho}) < \varepsilon\} \quad (8.1)$$

contains all the states that can be distinguished from $\hat{\rho}_0$ by an information effort smaller than that corresponding to the radius $\varepsilon > 0$. According to Jeffreys' rule [47], the size of the statistical inference region (8.1), which measures the uncertainty in the information acquired about the state $\hat{\rho}_0$, is precisely the Bures volume $\mathcal{V}_B[B_n(\hat{\rho}_0; \varepsilon)]$. Therefore, this volume can be interpreted as the *average statistical uncertainty* of the state $\hat{\rho}_0 \in (\mathcal{M}, g_B)$. In order to improve the accuracy in identifying the state $\hat{\rho}_0$, one has to contract the geodesic ball (8.1). Ideal asymptotic inference means reducing its radius as much as possible, that is, making $\varepsilon \rightarrow 0$. This asymptotic behaviour is described by the following geometric formula [64]:

$$\mathcal{V}_B[B_n(\hat{\rho}_0; \varepsilon)] = V_n(1) \varepsilon^n - \frac{V_n(1)}{n+2} R(\hat{\rho}_0) \varepsilon^{n+2} + o(\varepsilon^{n+2}) :$$

$$V_n(1) = \frac{\pi^{\frac{n}{2}}}{\Gamma(\frac{n}{2} + 1)}, \quad (\varepsilon \ll 1). \quad (8.2)$$

In Eq. (8.2), $V_n(1)$ is the volume of the unit ball $B_n(0; 1)$ in the Euclidean space \mathbb{R}^n , while $R(\hat{\rho}_0)$ denotes the Bures scalar curvature at the state $\hat{\rho}_0$. What Eq. (8.2) shows us is that, under the condition $\varepsilon \ll 1$, the average statistical uncertainty is fully determined by the scalar curvature $R(\hat{\rho}_0)$ and, namely, is a decreasing function of it.

To conclude, we come back to our four-dimensional Riemannian manifolds of special two-mode GSs,

$\mathcal{M}(\bar{n}_1, \bar{n}_2, \theta, \phi)$ and $\mathcal{M}(\bar{n}_1, \bar{n}_2, 2r, \phi)$. Figures 1 and 3, where their scalar curvatures are plotted, offer a global view on the average statistical uncertainty of these noteworthy states. Remark that almost all of them are noisy, except for the pure states, $(\bar{n}_1 = 0, \bar{n}_2 = 0)$, i. e., the vacuum and, respectively, all the two-mode SVSs. The figured values, albeit not completely intuitive, nevertheless display several regularities and provide some interesting comparisons. It is our opinion that these results urge a deeper understanding from a quantum information perspective.

Appendix A: Fidelity between n -mode Gaussian states: The inequality $\mathcal{F}(\hat{\rho}', \hat{\rho}'') \geq \text{Tr}(\hat{\rho}'\hat{\rho}'')$

We make a digression intended for a pair of arbitrary n -mode Gaussian states, $\hat{\rho}'$ and $\hat{\rho}''$. It is straightforward to extend Eqs. (3.7)- (3.10) to the multi-mode case [8]. Since the overlap $\text{Tr}(\hat{\rho}'\hat{\rho}'')$ of two GSs never vanishes, we have been lead to introduce a key GS [8],

$$\hat{\rho}_B := [\text{Tr}(\hat{\mathcal{B}})]^{-1}\hat{\mathcal{B}}, \quad \hat{\mathcal{B}} := \sqrt{\hat{\rho}''}\hat{\rho}'\sqrt{\hat{\rho}''}. \quad (\text{A1})$$

Its CM, denoted \mathcal{V}_B , has the symplectic invariants [8]:

$$\det(\mathcal{V}_B) = 2^{-2n}\frac{\Gamma}{\Delta}, \quad \det\left(\mathcal{V}_B + \frac{i}{2}J\right) = 2^{-2n}\frac{\Lambda}{\Delta}. \quad (\text{A2})$$

Obviously, the fidelity (2.7) of two GSs is proportional to their overlap given by an n -mode analogue of Eq. (3.10) [8]:

$$\mathcal{F}(\hat{\rho}', \hat{\rho}'') = \left[\text{Tr}\left(\sqrt{\hat{\rho}_B}\right)\right]^2 \text{Tr}(\hat{\rho}'\hat{\rho}'') > 0. \quad (\text{A3})$$

Equation (A3) displays the general inequality

$$\mathcal{F}(\hat{\rho}', \hat{\rho}'') \geq \text{Tr}(\hat{\rho}'\hat{\rho}''), \quad (\text{A4})$$

as well as its saturation, which is achieved if and only if the state $\hat{\rho}_B$ is pure:

$$\mathcal{F}(\hat{\rho}', \hat{\rho}'') = \text{Tr}(\hat{\rho}'\hat{\rho}'') \iff \text{Tr}\left[(\hat{\rho}_B)^2\right] = 1. \quad (\text{A5})$$

Owing to the formulae (A2), the purity condition (A5) reads

$$\mathcal{F}(\hat{\rho}', \hat{\rho}'') = \text{Tr}(\hat{\rho}'\hat{\rho}'') \iff \Gamma = \Delta, \quad (\text{A6})$$

and implies the equation

$$\det\left(\mathcal{V}_B + \frac{i}{2}J\right) = 0 \iff \Lambda = 0. \quad (\text{A7})$$

The necessary condition (A7) signifies that at least one of the GSs, for instance $\hat{\rho}'$, is at the physicality edge: $\det(\mathcal{V}' + \frac{i}{2}J) = 0$. Specifically, in the single-mode case ($n = 1$), the corresponding state $\hat{\rho}'$ is pure.

Conversely, if one of the above n -mode GSs, say $\hat{\rho}'$, is pure, then so is the GS $\hat{\rho}_B$, Eq. (A1). Indeed, the required equality $\Gamma = \Delta$ is a consequence of the assumed purity conditions $\det(\mathcal{V}') = 2^{-2n}$ and $\mathcal{V}' = -\frac{1}{4}J(\mathcal{V}')^{-1}J$ [8]. As shown in Sec. II, this sufficient condition for the saturation property $\mathcal{F}(\hat{\rho}', \hat{\rho}'') = \text{Tr}(\hat{\rho}'\hat{\rho}'')$ is a general one. We stress that, for single-mode GSs, it is both necessary and sufficient.

However, the one-mode case can readily be handled by making direct use of the explicit fidelity formula which is available for a long time [7]:

$$\mathcal{F}(\hat{\rho}', \hat{\rho}'') = \left(\sqrt{\Delta + \Lambda} - \sqrt{\Lambda}\right)^{-1} \times \exp\left[-\frac{1}{2}(\delta v)^T(\mathcal{V}' + \mathcal{V}'')^{-1}\delta v\right]. \quad (\text{A8})$$

Equation (A3) has the specific form

$$\mathcal{F}(\hat{\rho}', \hat{\rho}'') = \left(\sqrt{1 + \frac{\Lambda}{\Delta}} + \sqrt{\frac{\Lambda}{\Delta}}\right) \text{Tr}(\hat{\rho}'\hat{\rho}'') > 0. \quad (\text{A9})$$

Accordingly, the general inequality (A4) is manifest and so is the saturation condition

$$\mathcal{F}(\hat{\rho}', \hat{\rho}'') = \text{Tr}(\hat{\rho}'\hat{\rho}'') \iff \Lambda = 0, \quad (\text{A10})$$

meaning that at least one of the single-mode GSs $\hat{\rho}'$ and $\hat{\rho}''$ is pure.

Appendix B: Fidelity between thermal states: The inequality $\mathcal{F}(\hat{\rho}', \hat{\rho}'') \leq 1$

Let us introduce the positive function

$$\mathcal{Q}(x, y) := \sqrt{(x+1)(y+1)} - \sqrt{xy}, \quad (x \geq 0, y \geq 0). \quad (\text{B1})$$

Remark that the equivalent inequalities

$$(\sqrt{x} - \sqrt{y})^2 \geq 0 \iff \mathcal{Q}(x, y) \geq 1 \quad (\text{B2})$$

become saturate if and only if $x = y$:

$$\mathcal{Q}(x, y) = 1 \iff x = y. \quad (\text{B3})$$

1. Single-mode thermal states

A single-mode TS, $\hat{\rho}_T(\bar{n})$, is an unshifted GS whose explicit expression is written in Eq. (4.1). Recall that its 2×2 CM is a multiple of the identity:

$$\mathcal{V}_T(\bar{n}) = \left(\bar{n} + \frac{1}{2}\right)\sigma_0. \quad (\text{B4})$$

The fidelity (A8) of a pair of one-mode TSSs, $\hat{\rho}_T(\bar{n}')$ and $\hat{\rho}_T(\bar{n}'')$, is therefore

$$\mathcal{F}[\hat{\rho}_T(\bar{n}'), \hat{\rho}_T(\bar{n}'')] = \left(\sqrt{\Delta + \Lambda} - \sqrt{\Lambda} \right)^{-1} \quad (\text{B5})$$

with the determinants:

$$\Delta = (\bar{n}' + \bar{n}'' + 1)^2, \quad \Lambda = 4\bar{n}'(\bar{n}' + 1)\bar{n}''(\bar{n}'' + 1). \quad (\text{B6})$$

From Eqs. (B6) and (B1) we get the identity

$$\sqrt{\Delta + \Lambda} - \sqrt{\Lambda} = [\mathcal{Q}(\bar{n}', \bar{n}'')]^2 \quad (\text{B7})$$

and the fidelity (B5) reads thereby explicitly:

$$\mathcal{F}[\hat{\rho}_T(\bar{n}'), \hat{\rho}_T(\bar{n}'')] = [\mathcal{Q}(\bar{n}', \bar{n}'')]^{-2}. \quad (\text{B8})$$

Accordingly, Eq. (B2) displays the inequality

$$\mathcal{F}[\hat{\rho}_T(\bar{n}'), \hat{\rho}_T(\bar{n}'')] \leq 1, \quad (\text{B9})$$

while Eq. (B3) ascertains its saturation:

$$\mathcal{F}[\hat{\rho}_T(\bar{n}'), \hat{\rho}_T(\bar{n}'')] = 1 \iff \bar{n}' = \bar{n}''. \quad (\text{B10})$$

2. Two-mode thermal states

Let $K_{\pm}(\{\bar{n}\})$ designate the functions (3.12) for a pair of two-mode TSSs. They are limit cases of the similar functions for both corresponding pairs of MTSs and STSs. In order to write them, it is sufficient to set either $\theta' = \theta''$, $\phi' = \phi''$ in Eq. (5.6) or $r' = r''$, $\phi' = \phi''$ in Eq. (5.10):

$$K_+(\{\bar{n}\}) = 2 \left\{ (\bar{n}'_1 \bar{n}'_2 \bar{n}''_1 \bar{n}''_2)^{\frac{1}{2}} + [(\bar{n}'_1 + 1)(\bar{n}'_2 + 1)(\bar{n}''_1 + 1)(\bar{n}''_2 + 1)]^{\frac{1}{2}} \right\}^2. \quad (\text{B11})$$

$$K_-(\{\bar{n}\}) = 2 \left\{ [\bar{n}'_1(\bar{n}'_2 + 1)\bar{n}''_1(\bar{n}''_2 + 1)]^{\frac{1}{2}} + [(\bar{n}'_1 + 1)\bar{n}'_2(\bar{n}''_1 + 1)\bar{n}''_2]^{\frac{1}{2}} \right\}^2. \quad (\text{B12})$$

The difference between the square roots of the above functions factors as follows:

$$\begin{aligned} & \sqrt{K_+(\{\bar{n}\})} - \sqrt{K_-(\{\bar{n}\})} \\ &= \sqrt{2} \mathcal{Q}(\bar{n}'_1, \bar{n}''_1) \mathcal{Q}(\bar{n}'_2, \bar{n}''_2). \end{aligned} \quad (\text{B13})$$

Substitution of Eq. (B13) into Eq. (5.1) gives the fidelity of a pair of two-mode TSSs:

$$\begin{aligned} & \mathcal{F}[\hat{\rho}_T(\bar{n}'_1, \bar{n}'_2), \hat{\rho}_T(\bar{n}''_1, \bar{n}''_2)] \\ &= [\mathcal{Q}(\bar{n}'_1, \bar{n}''_1) \mathcal{Q}(\bar{n}'_2, \bar{n}''_2)]^{-2}. \end{aligned} \quad (\text{B14})$$

Equation (B2) confirms therefore the inequality

$$\mathcal{F}[\hat{\rho}_T(\bar{n}'_1, \bar{n}'_2), \hat{\rho}_T(\bar{n}''_1, \bar{n}''_2)] \leq 1, \quad (\text{B15})$$

which saturates as stated by Eq. (B3):

$$\begin{aligned} & \mathcal{F}[\hat{\rho}_T(\bar{n}'_1, \bar{n}'_2), \hat{\rho}_T(\bar{n}''_1, \bar{n}''_2)] = 1 \iff \bar{n}'_j = \bar{n}''_j, \\ & (j = 1, 2). \end{aligned} \quad (\text{B16})$$

Taking account of the formula (B8) for one-mode TSSs, the structure (B14) of the fidelity between two-mode TSSs (4.1) checks the multiplicativity of fidelity in this particular case. The reason for which the formulae (B14)- (B16) can be extended to n -mode TSSs, regardless of the number of modes, is precisely the above-mentioned multiplication rule.

Appendix C: Fidelity of special two-mode Gaussian states: The inequality $\mathcal{F}(\hat{\rho}', \hat{\rho}'') \leq 1$

In addition to a pair of special two-mode GSs of the same kind, $\hat{\rho}'$ and $\hat{\rho}''$, we envisage the pair of two-mode TSSs, $\hat{\rho}'_T$ and $\hat{\rho}''_T$, with the same mean thermal photon occupancies: $\{\bar{n}'_1, \bar{n}'_2\}$ and $\{\bar{n}''_1, \bar{n}''_2\}$, respectively.

1. Mode-mixed thermal states

We define the MTSs $\hat{\rho}'_{\text{MT}}$ and $\hat{\rho}''_{\text{MT}}$ by the sets of their usual parameters, $\{\bar{n}'_1, \bar{n}'_2, \theta', \phi'\}$ and $\{\bar{n}''_1, \bar{n}''_2, \theta'', \phi''\}$, respectively. Inspection of Eqs. (5.5)- (5.6) and (B11)- (B12) provides the identities:

$$\begin{aligned} & K_+ = K_+(\{\bar{n}\}), \quad K_- = K_-(\{\bar{n}\}) \\ & - (\bar{n}'_1 - \bar{n}'_2)(\bar{n}''_1 - \bar{n}''_2) \{1 - \cos(\theta' - \theta'') \\ & + \sin(\theta') \sin(\theta'') [1 - \cos(\phi' - \phi'')]\}. \end{aligned} \quad (\text{C1})$$

The emerging inequality

$$\sqrt{K_+} - \sqrt{K_-} \geq \sqrt{K_+(\{\bar{n}\})} - \sqrt{K_-(\{\bar{n}\})} \quad (\text{C2})$$

generates via Eq. (5.1) an inequality for fidelities,

$$\mathcal{F}(\hat{\rho}'_{\text{MT}}, \hat{\rho}''_{\text{MT}}) \leq \mathcal{F}[\hat{\rho}_T(\bar{n}'_1, \bar{n}'_2), \hat{\rho}_T(\bar{n}''_1, \bar{n}''_2)], \quad (\text{C3})$$

with the saturation condition

$$\begin{aligned} & \mathcal{F}(\hat{\rho}'_{\text{MT}}, \hat{\rho}''_{\text{MT}}) = \mathcal{F}[\hat{\rho}_T(\bar{n}'_1, \bar{n}'_2), \hat{\rho}_T(\bar{n}''_1, \bar{n}''_2)] \\ & \iff \theta' = \theta'', \phi' = \phi''. \end{aligned} \quad (\text{C4})$$

By use of Eqs. (C3)- (C4) and (B15)- (B16), we get the expected property (2.9) for MTSs, that is, the inequality

$$\mathcal{F}(\hat{\rho}'_{\text{MT}}, \hat{\rho}''_{\text{MT}}) \leq 1 \quad (\text{C5})$$

and its saturation condition as well:

$$\mathcal{F}(\hat{\rho}'_{\text{MT}}, \hat{\rho}''_{\text{MT}}) = 1 \iff \hat{\rho}'_{\text{MT}} = \hat{\rho}''_{\text{MT}}. \quad (\text{C6})$$

2. Squeezed thermal states

Let $\{\bar{n}'_1, \bar{n}'_2, r', \phi'\}$ and $\{\bar{n}''_1, \bar{n}''_2, r'', \phi''\}$ be the parameters of the STSs $\hat{\rho}'_{\text{ST}}$ and $\hat{\rho}''_{\text{ST}}$, respectively. By looking at Eqs. (5.10)- (5.11) and (B11)- (B12), we get the formulae:

$$\begin{aligned} K_+ &= K_+(\{\bar{n}\}) \\ &+ (\bar{n}'_1 + \bar{n}'_2 + 1)(\bar{n}''_1 + \bar{n}''_2 + 1) \{ \cosh[2(r' - r'')] - 1 \\ &+ \sinh(2r') \sinh(2r'') [1 - \cos(\phi' - \phi'')] \}, \\ K_- &= K_-(\{\bar{n}\}) \end{aligned} \quad (\text{C7})$$

The obvious inequality

$$\sqrt{K_+} - \sqrt{K_-} \geq \sqrt{K_+(\{\bar{n}\})} - \sqrt{K_-(\{\bar{n}\})} \quad (\text{C8})$$

gives rise, via Eq. (5.1), to an inequality for fidelities,

$$\mathcal{F}(\hat{\rho}'_{\text{ST}}, \hat{\rho}''_{\text{ST}}) \leq \mathcal{F}[\hat{\rho}_{\text{T}}(\bar{n}'_1, \bar{n}'_2), \hat{\rho}_{\text{T}}(\bar{n}''_1, \bar{n}''_2)], \quad (\text{C9})$$

with the saturation case

$$\begin{aligned} \mathcal{F}(\hat{\rho}'_{\text{ST}}, \hat{\rho}''_{\text{ST}}) &= \mathcal{F}[\hat{\rho}_{\text{T}}(\bar{n}'_1, \bar{n}'_2), \hat{\rho}_{\text{T}}(\bar{n}''_1, \bar{n}''_2)] \\ \iff r' &= r'', \phi' = \phi''. \end{aligned} \quad (\text{C10})$$

By making combined use of Eqs. (C9)- (C10) together with Eqs. (B15)- (B16), we get the expected property (2.9) for STSs, consisting of the inequality

$$\mathcal{F}(\hat{\rho}'_{\text{ST}}, \hat{\rho}''_{\text{ST}}) \leq 1 \quad (\text{C11})$$

and its saturation case:

$$\mathcal{F}(\hat{\rho}'_{\text{ST}}, \hat{\rho}''_{\text{ST}}) = 1 \iff \hat{\rho}'_{\text{ST}} = \hat{\rho}''_{\text{ST}}. \quad (\text{C12})$$

Acknowledgments This work was supported by the Romanian National Authority for Scientific Research, CNCS-UEFISCDI, through Project PN-II-ID-PCE-2011-3-1012 for the University of Bucharest.

-
- [1] M. A. Nielsen and I. L. Chuang, *Quantum Computation and Quantum Information* (Cambridge University Press, Cambridge, UK, 2000).
- [2] I. Bengtsson and K. Życzkowski, *Geometry of Quantum States: An Introduction to Quantum Entanglement* (Cambridge University Press, Cambridge, UK, 2006).
- [3] A. Furusawa, J. L. Sørensen, S. L. Braunstein, C. A. Fuchs, H. J. Kimble, and E. S. Polzik, *Science* **282**, 706 (1998).
- [4] S. Olivares, *Eur. Phys. J. Special Topics* **203**, 3 (2012).
- [5] C. Weedbrook, S. Pirandola, R. García-Patrón, N. J. Cerf, T. C. Ralph, J. H. Shapiro, S. Lloyd, *Rev. Mod. Phys.* **84**, 621 (2012).
- [6] G. Adesso, S. Ragy, and A. R. Lee, *Open System Inf. Dyn.* **21**, 1440001 (2014).
- [7] H. Scutaru, *J. Phys. A: Math. Gen.* **31**, 3659 (1998).
- [8] Paulina Marian and T. A. Marian, *Phys. Rev. A* **86**, 022340 (2012).
- [9] A. Bhattacharyya, *Bull. Calcutta Math. Soc.* **35**, 99 (1943).
- [10] W. K. Wootters, *Phys. Rev. D* **23**, 357 (1981).
- [11] C. A. Fuchs and C. M. Caves, *Open System Inf. Dyn.* **3**, 345 (1995).
- [12] S. Luo and Q. Zhang, *Phys. Rev. A* **69**, 032106 (2004).
- [13] D. Bures, *Trans. Am. Math. Soc.* **135**, 199 (1969).
- [14] A. Uhlmann, *Rep. Math. Phys.* **9**, 273 (1976).
- [15] R. Jozsa, *J. Mod. Opt.* **41**, 2315 (1994).
- [16] C. A. Fuchs, Ph. D. Thesis, University of New Mexico (1995).
- [17] H. Barnum, C. M. Caves, C. A. Fuchs, R. Jozsa, and B. Schumacher, *Phys. Rev. Lett.* **76**, 2818 (1996).
- [18] Paulina Marian and T. A. Marian, *J. Phys. A: Math. Theor.* **48**, 115301 (2015).
- [19] P. E. M. F. Mendonça, R. d. J. Napolitano, M. A. Marchioli, C. J. Foster, and Y.-C. Liang, *Phys. Rev. A* **78**, 052330 (2008).
- [20] M. Hübner, *Phys. Lett. A* **163**, 239 (1992).
- [21] S. L. Braunstein and C. M. Caves, *Phys. Rev. Lett.* **72**, 3439 (1994).
- [22] D. Petz and C. Sudár, *J. Math. Phys.* **37**, 2662 (1996).
- [23] H.-J. Sommers and K. Życzkowski, *J. Phys. A: Math. Gen.* **36**, 10083 (2003).
- [24] R. Simon, E.C.G. Sudarshan, and N. Mukunda, *Phys. Rev. A* **36**, 3868 (1987).
- [25] H. Scutaru, *Phys. Lett. A* **141**, 223 (1989).
- [26] R. Simon, N. Mukunda, and B. Dutta, *Phys. Rev. A* **49**, 1567 (1994).
- [27] U. Leonhardt, *Essential Quantum Optics. From Quantum Measurements to Black Holes*, (Cambridge University Press, Cambridge, UK, 2010).
- [28] Lu-Ming Duan, G. Giedke, J. I. Cirac, and P. Zoller, *Phys. Rev. Lett.* **84**, 2722 (2000).
- [29] Bonny L. Schumaker, *Phys. Reports* **135**, 317 (1986).
- [30] P. Jordan, *Z. Physik* **94**, 531 (1935).
- [31] J. Schwinger, *On Angular Momentum* (U. S. Atomic Energy Commission Report NYO-3071, 1952, unpublished). Reprinted in *Quantum Theory of Angular Momentum* (L. C. Biedenharn and H. van Dam, Eds.), pp. 229-279, (Academic Press, New York, 1965).
- [32] J. M. Radcliffe, *J. Phys. A: Gen. Phys.* **4**, 313 (1971).
- [33] F. T. Arecchi, E. Courtens, R. Gilmore, and H. Thomas, *Phys. Rev. A* **6**, 2211 (1972).
- [34] Bonny L. Schumaker and C. M. Caves, *Phys. Rev. A* **31**, 3093 (1985).
- [35] C. C. Gerry and P. L. Knight, *Introductory Quantum Optics* (Cambridge University Press, Cambridge, UK, 2005).
- [36] B. Yurke, S. L. McCall, and J. R. Klauder, *Phys. Rev. A* **33**, 4033 (1986).
- [37] L. C. Biedenharn and J. D. Louck, *The Racah-Wigner Algebra in Quantum Theory* (Addison-Wesley, Reading,

- Massachusetts, 1981). See pp. 275-281.
- [38] C. Brif, *Int. J. Theor. Phys.* **36**, 1651 (1997).
- [39] M. Novaes, *Revista Brasileira de Ensino de Física* **26**, 351 (2004). We have chosen the phase of ζ as in this brief review in order to let the complex variable $\lambda := e^{i\phi} \tanh(\frac{\tau}{2})$ parametrize the Perelomov $SU(1, 1)$ coherent states.
- [40] Paulina Marian, T. A. Marian, and H. Scutaru, *J. Phys. A: Math. Gen.* **34**, 6969 (2001).
- [41] Paulina Marian, T. A. Marian, and H. Scutaru, *Phys. Rev. A* **68**, 062309 (2003). See Eqs. (4.1), (4.9), and (4.10) therein.
- [42] J. Twamley, *J. Phys. A: Math. Gen.* **29**, 3723 (1996).
- [43] Gh.-S. Păraoanu and H. Scutaru, *Phys. Rev. A* **58**, 869 (1998).
- [44] O. Pinel, P. Jian, N. Treps, C. Fabre, and D. Braun, *Phys. Rev. A* **88**, 040102(R) (2013).
- [45] P. B. Slater, *J. Phys. A: Math. Gen.* **29**, L601 (1996).
- [46] C. M. Caves, C.A. Fuchs, and R. Schack, *J. Math. Phys.* **43**, 4537 (2002).
- [47] R. E. Kass, *Stat. Sci.* **4**, 188 (1989).
- [48] The stereographic projection of H^2_1 from the south pole $(0, 0, -1)$ into the plane $z = 0$ is the open unit disk $D^2 := \{(x, y) \mid x^2 + y^2 < 1\}$. This map is an isometry connecting two analytic representations of the hyperbolic plane H^2 : the hyperboloid model H^2_1 and the Poincaré disk model D^2 . The latter is presented in H. S. M. Coxeter, *Introduction to Geometry*, Second Edition, Chapter 16 (Wiley, New York, 1989).
- [49] J. W. Cannon, W. J. Floyd, R. Kenyon, and W. R. Parry, *Hyperbolic Geometry*, pp. 59-115, in *Flavors of Geometry*, edited by S. Levy, MSRI Publications **31** (Cambridge University Press, Cambridge, UK, 1997).
- [50] G. Adesso, *Phys. Rev. A* **90**, 022321 (2014).
- [51] D. Šafránek, A. R. Lee, and Ivette Fuentes, *New J. Phys.* **17**, 073016 (2015).
- [52] M. Ahmadi, D.E. Bruschi, C. Sabín, G. Adesso, and Ivette Fuentes, *Scientific Reports* **4**, 4996 (2014).
- [53] M. Ahmadi, D.E. Bruschi, and Ivette Fuentes, *Phys. Rev. D* **89**, 065028 (2014).
- [54] M. G. A. Paris, *Int. J. Quantum Inf.* **7**, 125 (2009).
- [55] M. G. Genoni, P. Giorda, and M. G. A. Paris, *Phys. Rev. A* **78**, 032303 (2008).
- [56] A. Monras and F. Illuminati, *Phys. Rev. A* **81**, 062326 (2010).
- [57] A. Monras, *Phase space formalism for quantum estimation of Gaussian states*, arXiv:1303.3682.
- [58] Z. Jiang, *Phys. Rev. A* **89**, 032128 (2014). The QFI formula, Eq. (4.29) therein, is in agreement with the similar formula, Eq. (B.10), in Ref. [57].
- [59] M. P. do Carmo, *Riemannian Geometry* (Birkhäuser, Boston, Massachusetts, 1992).
- [60] The corresponding principal curvatures at the saddle point S are $k_1 \approx -4.19$ and $k_2 \approx 10.09$. Their product, $K := k_1 k_2 \approx -42.31$, is the Gaussian curvature of the surface at its saddle point S .
- [61] R. L. Bishop and B. O'Neill, *Trans. Amer. Math. Soc.* **145**, 1 (1969).
- [62] F. Dobarro and E. Lami Dozo, *Trans. Amer. Math. Soc.* **303**, 161 (1987). See Theorem 2.1 therein.
- [63] D. Petz, *J. Phys. A: Math. Gen.* **35**, 929 (2002).
- [64] S. Gallot, D. Hulin, and J. Lafontaine, *Riemannian Geometry*, Third Edition (Springer, Berlin, 2004). See Theorem 3.98, p. 168.